Biomaterials Science

ROYAL SOCIETY OF CHEMISTRY

REVIEW

View Article Online
View Journal | View Issue

Cite this: *Biomater. Sci.*, 2025, **13**, 1624

Microfluidic organ-on-a-chip models for the gut–liver axis: from structural mimicry to functional insights

Wanlin Hu,†[a,b] Yushen Wang,†[a,b] Junlei Han,[a,b] Wenhong Zhang,[c] Jun Chen,[a,b] Xinyu Li*[d] and Li Wang *[a,b]

The gut–liver axis plays a crucial role in maintaining metabolic balance and overall human health. It orchestrates various processes, such as blood flow, nutrient transfer, metabolite processing, and immune cell communication between the two organs. Traditional methods, such as animal models and two-dimensional (2D) cell cultures, are insufficient in fully replicating the intricate functions of the gut–liver axis. The emergence of microfluidic technology has revolutionized this field, facilitating the development of organ-on-a-chip (OOC) systems. These systems are capable of mimicking the complex structures and dynamic environments of the gut and liver *in vitro* and incorporating sensors for real-time monitoring. In this article, we review the latest progress in gut-on-a-chip (GOC) and liver-on-a-chip (LOC) systems, as well as the integrated gut–liver-on-a-chip (GLOC) models. Our focus lies in the simulation of physiological parameters, three-dimensional (3D) structural mimicry, microbiome integration, and multicellular co-culture. All these aspects are essential for constructing accurate *in vitro* models of the gut and liver. Furthermore, we explore the current applications of OOC technology in the study of the gut and liver, including its use in disease modeling, toxicity testing, and drug screening. Finally, we discuss the challenges that remain and outline potential future directions for advancing GOC and LOC development *in vitro*.

Received 24th September 2024,
Accepted 26th January 2025

DOI: 10.1039/d4bm01273a

rsc.li/biomaterials-science

1. Introduction

The gut–liver axis denotes the bidirectional interaction between the gut, including its microbiome, and the liver. This interaction is essential for maintaining metabolic balance and overall health in humans. Venous blood from the gut is directed to the liver *via* the portal vein, which supplies approximately 75% of the liver's blood flow.[1] In parallel, various nutrients, metabolites, and toxins from the gut are transported to the liver, where they undergo further metabolism and detoxification.[2] Furthermore, bile secreted by the liver not only facilitates fat digestion but also efficiently recycles and reuses bile salts through the enterohepatic circulation.[3]

Metabolites produced by the gut microbiota directly influence liver function and health, while immune cell interactions between the gut and liver play a key role in regulating systemic inflammatory responses.[4] Dysregulation of the gut–liver axis is closely associated with various diseases, such as non-alcoholic fatty liver disease (NAFLD) and inflammatory bowel disease (IBD), where a vicious cycle of gut barrier dysfunction and hepatic impairment accelerates disease progression.[5,6] The link between metabolic syndrome and alterations in gut microbiota and liver function is particularly pronounced. Dysbiosis, specifically an abnormal ratio of Firmicutes to Bacteroidetes, affects lipid and glucose metabolism, decreases insulin sensitivity, and compromises gut barrier integrity, leading to endotoxins entering the portal system, which activates hepatic inflammation and exacerbates liver injury.[7,8] These changes place an increased metabolic burden on the liver, particularly under conditions of bile acid dysregulation, further deteriorating liver function and driving the progression of metabolic syndrome.[9,10] Therefore, an in-depth investigation of the physiological connections within the gut–liver axis is essential for uncovering disease pathogenesis and advancing therapeutic strategies.

With advances in biomedical research, there is an increasing demand for precise *in vitro* simulations of human

[a]*School of Mechanical Engineering, Qilu University of Technology (Shandong Academy of Sciences), Jinan 250353, China. E-mail: liwang@qlu.edu.cn*
[b]*Shandong Institute of Mechanical Design and Research, Jinan 250353, China*
[c]*College of Mechanical Engineering, Donghua University, Shanghai 201620, China*
[d]*Department of Minimally Invasive Comprehensive Treatment of Cancer, Shandong Provincial Hospital Affiliated to Shandong First Medical University, Jinan, Shandong, 250021, China. E-mail: lixinyu@sdfmu.edu.cn*
†Wanlin Hu and Yushen Wang contributed equally to this work and should be considered co-first authors.

physiological conditions. The importance of faithfully replicating the human environment *in vitro* is now widely recognized across drug development, disease mechanism research, and personalized medicine applications.[11,12] Although traditional animal models and two-dimensional (2D) cell cultures have provided valuable data for scientific research, they face significant limitations in replicating the complexity of human physiology.[13] The substantial biological differences between animals and humans hinder the translation of findings to human physiology. Additionally, the establishment and maintenance of animal models are not only costly but also raise ethical and animal welfare concerns.[14–16] In contrast, 2D cultures fail to replicate the three-dimensional (3D) tissue structures and dynamic environments essential to capture organ functionality fully. Thus, the development of novel *in vitro* models that can accurately mimic the human physiological environment has become increasingly urgent.[17]

The advancements in microfabrication and microfluidics have significantly accelerated the development of organ-on-a-chip (OOC) systems for biological analysis. These chips have made remarkable progress in studying human microphysiological systems *in vitro*, enabling the replication of organ-level and even organism-level functions.[18] Compared with traditional animal models, OOC systems offer notable ethical advantages and provide a more accurate simulation of human organ physiology.[19] Furthermore, by integrating human-relevant cells into these OOC platforms, researchers can investigate key gut–liver functions within 3D structures and physiological microenvironments that closely resemble natural human tissues.[20–22] These culture systems enable dynamic cultivation by precisely controlling fluid flow and introducing metabolites, drugs, and nutrients. This approach replicates the range of fluid movement and associated shear stresses experienced by cells within human gut lumens and capillaries.[23] Additionally, OOC systems can be integrated with various sensors to enable real-time monitoring of cellular and tissue-level activities and simulate pathological conditions.[24,25] As pivotal organs in the digestive system, the advancement of this technology has dramatically enhanced research into gut and liver diseases, as well as drug screening. With appropriate design, gut–liver-on-a-chip (GLOC) systems can replicate the bidirectional connectivity between the gut and liver *in vitro* while maintaining the viability and functionality of both gut and liver cells.[26] These technologies offer more accurate *in vitro* models by replicating the complex structures and dynamic environments of organs such as the intestine and liver.

This review focuses on recent advances in gut-on-a-chip (GOC) and liver-on-a-chip (LOC) systems and integrated GLOC models. We aim to evaluate the achievements of these systems in simulating physiological parameters, biomimetic 3D structures, microbiome integration, and multicellular co-culture. Additionally, we explore their applications in disease modeling, toxicity testing, and drug transport. The review also addresses current challenges and offers potential research directions for the future development of GOC and LOC technologies. However, it does not cover quantitative *in vitro–in vivo* extrapolation (IVIVE) or detailed computational modeling approaches, which are beyond the scope of this discussion.

2. Gut-on-a-chip

2.1 The design principles of gut models

A comprehensive understanding of the gut's structure and function is pivotal for the effective design of the chip's internal components (Fig. 1a and b).[27] The gut is a lengthy, cylindrical organ, with an approximate surface area of 100 square meters, primarily due to the extensive folding of intestinal villi and microvilli.[28] This architecture increases the absorptive surface area and provides a complex biophysical environment for cellular interactions. The intestinal epithelium is composed of diverse cell types, with a protective mucus layer that serves as a barrier, separating the microbe- and nutrient-rich gut lumen from the largely sterile underlying tissues.[29] Columnar epithelial cells are the predominant cell type within this epithelium (Fig. 1b), playing a key role in regulating the diffusion of small molecules and preventing the entry of toxic macromolecules *via* tight junctions.[30] Therefore, the integrity of the gut barrier, encompassing the epithelium and mucosa, is essential for maintaining physiological homeostasis within the gastrointestinal tract.[6] This barrier prevents the uncontrolled passage of compounds and microorganisms, thus protecting the body from harmful substances and pathogens.[31] Meanwhile, the gut experiences mechanical stress from peristaltic movements, which stretch and compress tissues, facilitating the propulsion of contents through the gastrointestinal tract. These movements not only aid in food and waste transport but also modulate the concentration of antimicrobial compounds. In addition, the gut harbors a vital microbiota that plays essential roles in digestion and metabolism. This microbiota helps degrade indigestible fibers and produces crucial metabolites, such as short-chain fatty acids and secondary bile acids.[32] The gut microbiota and its metabolites are fundamental to maintaining gut health, regulating the immune system, and influencing the development of both gut-related and systemic diseases.[33,34] Within this complex physiological environment, the small and large intestines maintain a steep oxygen gradient, ranging from aerobic conditions at the epithelial surface to anaerobic conditions in the lumen, thereby creating an optimal environment for the proliferation of anaerobic microbiota.[35] The presence of this oxygen gradient further supports the diversity and metabolic activity of the intestinal microbiota, highlighting the complexity of intestinal functions.

The intestine is not only the primary site for nutrient absorption but also a crucial endocrine and immune organ, playing a central role in maintaining systemic metabolic balance and overall health. As the body's largest endocrine organ, intestinal enteroendocrine cells secrete various hormones, such as glucagon-like peptide-1 (GLP-1) and gastric inhibitory peptide (GIP), to regulate glucose homeostasis, gas-

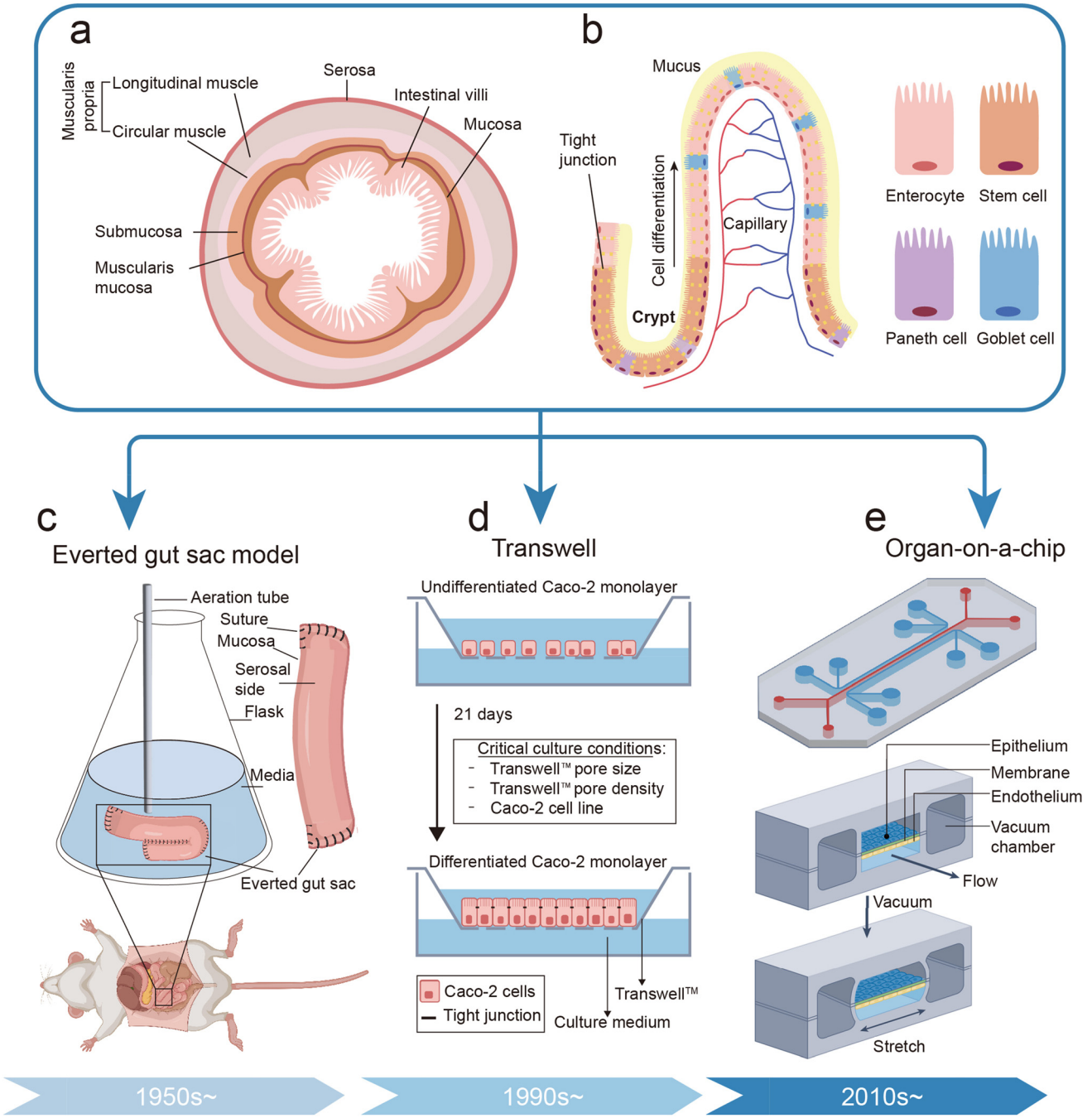

Fig. 1 Advances in developing gut architecture and corresponding *in vitro* models. (a) A cross-sectional representation of the small intestine. Delineating the distinct layers: the mucosa, submucosa, muscularis (comprising both circular and longitudinal muscle layers), and serosa. (Reprinted with permission from ref. 27. Copyright 2023, John Wiley and Sons). (b) Schematic illustration of the small intestine architecture. Columnar epithelial cells are interconnected by tight junctions, establishing the primary barrier function of the intestinal epithelium. (c) Everted gut sac model. Originally introduced in the mid-1950s, the everted gut sac model has undergone continuous modification and refinement to improve tissue viability and preserve the integrity of the mucosal epithelium. (d) Transwell culture model. First proposed in the early 1990s for the *in vitro* cultivation of Caco-2 cells, the Transwell system enables these cells to differentiate into a monolayer that mimics the small intestinal epithelium. (e) Schematic diagram of OOC. The emergence of OOC technology offers cutting-edge tools for investigating gut physiological functions. (Reprinted with permission from ref. 18. Copyright 2022, Springer Nature).

trointestinal motility, and satiety.[36] In terms of immune function, the intestine houses the largest immune system in the body, enriched with gut-associated lymphoid tissue (GALT), which maintains a dynamic balance through complex interactions with the gut microbiota and external antigens.[37] The intestinal immune system not only effectively defends against pathogens but also establishes immune tolerance to prevent aberrant reactions to dietary components and commensal

microbes. Disruption of this balance, however, can lead to pathological conditions such as inflammatory bowel diseases, autoimmune disorders, and food allergies.

Caco-2 cells, derived from human colorectal adenocarcinoma, are widely utilized *in vitro* due to their ability to spontaneously differentiate into a monolayer structure resembling the small intestinal epithelium during cultivation.[38] This monolayer exhibits key characteristics such as apical brush border microvilli, tight junction proteins, and brush border enzymes, making it an essential model for studying intestinal absorption, transport, and barrier functions.[39] These attributes have positioned Caco-2 cells as a pivotal tool in pharmacokinetics, toxicology, and the elucidation of intestinal disease mechanisms. However, the Caco-2 cell model is not without limitations. For instance, the degree of differentiation and polarization can vary depending on culture conditions, and the expression levels of certain transporters or metabolic enzymes may differ significantly from those in primary intestinal epithelial cells.[40] Additionally, the absence of enteroendocrine cell populations and associated signaling pathways limits the model's ability to replicate the complex intestinal microenvironment fully. This is particularly evident when investigating intestinal immune regulation or host–microbiota interactions, where using a single-cell type may fail to accurately reflect physiological or pathological processes.[41] To address these limitations, researchers have been developing more sophisticated models. Co-culturing Caco-2 cells with other cell types, such as immune cells or goblet cells, enables a more comprehensive representation of the intestinal multicellular composition.[42] Furthermore, advancements in 3D culture techniques and microfluidic chip technology have facilitated the construction of dynamic models featuring villus-like structures, providing environments that more closely mimic physiological conditions. These innovative strategies significantly enhance the utility of Caco-2 cell models in intestinal research, offering crucial support for deeper insights into intestinal physiology and pathophysiology.

Early researchers developed the gut ring model and the everted gut sac model for the *in vitro* cultivation and investigation of living gut tissue (Fig. 1c).[43,44] However, the absence of normal physiological conditions, such as pH and temperature, limited tissue viability in both models to less than two hours. In recent decades, researchers have commonly cultured human small intestinal epithelial cell lines, such as Caco-2 cells, on porous membranes coated with extracellular matrix (ECM) within Transwell chambers to establish human intestinal monolayers (Fig. 1d).[45] Transwell chambers' ease of mass production and operational convenience have significantly advanced research on intestinal cells. However, this 2D culture model fails to replicate the 3D architecture of natural tissues, lacking intrinsic gut features such as villus structures (surface area), peristaltic function, radial contraction, shear stress microenvironments, and other inherent multimodal movements and micromechanical environments.[46–51] Additionally, 2D systems struggle to capture the complex physiological features of the intestinal tract *in vivo*, including the expression patterns of drug-metabolizing enzymes and the coordinated interactions among various intestinal cell types.[52,53] In recent years, advancements in microfabrication and microfluidic technologies have facilitated the development of OOC systems.[54,55] These systems incorporate essential features of organs, including tissue differentiation, tissue–tissue interfaces, fluid dynamics, and mechanical stress.[56] This technology integrates microfluidics, dynamic tissue culture, micro/nanofabrication, and cell biology to simulate human organs using innovative reductionist approaches.[57–60] It deconstructs complex organs into their essential cellular microenvironments (Fig. 1e).[18]

As an emerging *in vitro* model, GOC can recapitulate the structure and function of the human intestine with high fidelity, offering an innovative platform for studying intestinal physiology, pathology, and drug evaluation.[61] Among its key features, intestinal barrier function is a core characteristic. By seeding polarized intestinal epithelial cells onto a porous membrane within a microfluidic chip, the tight junctions and selective permeability of the intestinal epithelium were successfully reconstructed.[62,63] Additionally, incorporating a dynamic fluidic environment provides shear stress to maintain physiological cellular states and significantly enhances the efficiency of nutrient exchange and metabolic waste removal.[64] Compared with traditional 2D culture methods, this dynamic co-culture system integrates intestinal epithelial cells, immune cells, and microbial communities, accurately replicating the intestinal microecology and its interactions with the host.[65] This high-fidelity microphysiological environment is a robust tool for investigating host–microbiota interactions, inflammatory mechanisms, and intestinal diseases such as IBD and leaky gut syndrome. Furthermore, the application of GOC in drug development has garnered widespread attention. Through the precise design of dynamic flow channels, the model enables the evaluation of drug absorption and metabolism within the intestine and the screening of potential toxic reactions.[18] With continuous technological advancements, future GOC are expected to incorporate more complex tissue structures and diverse cell types, further enhancing their ability to simulate the human intestine. This progress will provide a stronger foundation for studying intestinal diseases and developing therapeutic strategies.

Current GOC systems can be categorized into several types based on biomimetic design: first, the replication of physiological parameters, including mechanical strains related to peristalsis, shear stress generated by fluid flow, and oxygen concentration; second, the construction of chip microstructures, such as 3D ring-like configurations and protrusions that mimic intestinal villi; and third, the diversification of cell types, incorporating capillary endothelial cells, immune cells, and even symbiotic microbial cells for co-cultivation, thereby replicating the complex cellular interactions within the gut. In the following sections, we will review the progress of microfluidic chip technology in the study of bionic gut structure and function, while analyzing the limitations and challenges of current research.

2.2 *In vitro* biomimetic gut structure and function on microfluidic chips

2.2.1 Simulation of physiological parameters: mechanical stimulation and oxygen environment. Mechanical stimulation and anaerobic environments are essential elements in the design of GOC systems for the *in vitro* simulation of the gut. Mechanical stimulation encompasses shear stress from fluid flow and mechanical deformation resulting from peristaltic movements. These factors effectively mimic the fluid dynamics, cyclic motility, and anaerobic conditions of the human gut—conditions that traditional 2D cultures fail to replicate. Ramadan *et al.* developed a dynamic microfluidic intestinal barrier model by co-culturing Caco-2 cells with U937 cells (a human monocyte-derived cell line) to investigate immune responses and barrier function.[66] This model allows precise control of shear stress by adjusting fluid flow rates and utilizes a perfusion-based medium delivery system to supply clear soluble molecules within the extracellular microenvironment. The study revealed that the cells exhibited higher survival rates under perfusion conditions and increased transepithelial electrical resistance (TEER) values, which were closely associated with the cells' ability to adapt to fluid shear stress through mechanotransduction. Additionally, the Caco-2 monolayer in the co-culture system effectively suppressed the secretion of the pro-inflammatory cytokine TNF-α by U937 cells, further emphasizing its pivotal role in maintaining intestinal barrier function and defending against foreign pathogens or toxic substances. To gain a deeper understanding of the impact of shear stress on cellular function in intestinal barrier models, Fois *et al.* utilized computational fluid dynamics (CFD) simulations to predict the impact of shear stress on Caco-2 cell differentiation and morphology within colon-on-a-chip (COC) systems (Fig. 2a).[67] The model was constructed based on the typical dimensions of Caco-2 cells to demonstrate shear stress distribution across varying morphologies of Caco-2 cells under different flow conditions. The study used CFD simulations to analyze shear stress at both the single-cell level and within cell arrays in microchannels. The results indicated that the model provided a good approximation only at smaller cell sizes. The findings reveal that maintaining consistent cellular shear stress is critical for accurately simulating the *in vivo* intestinal environment and promoting cell polarization. In addition, Chi *et al.* emphasized the significance of mechanical stimulation on cellular functions.[46] Their study found that, compared with the Transwell model, fluid flow conditions led to the upregulation of mucin-2 (MUC-2) and actin expression, significantly reducing the number of adherent *E. coli* in the system.

Peristalsis, a distinct physiological activity resulting from gastrointestinal muscle contractions, is also essential to simulate alongside fluid shear stress. Modeling the periodic mechanical deformation experienced by intestinal tissue during peristalsis offers a more accurate representation of the gut's physical environment, providing deeper insights into its role in maintaining intestinal health and function. Kim *et al.* developed a sophisticated microfluidic dual-channel GOC system that enables human intestinal epithelial cells, capillary endothelial cells, immune cells, and even symbiotic microorganisms to grow, coexist, and interact under physiologically relevant conditions of fluid flow and peristaltic mechanical deformation.[70] This design replicates the complex gut environment and offers a more precise and physiologically relevant platform for studying cellular interactions and responses. In this model, Caco-2 cells cultured on the chip can spontaneously differentiate into various cell types, including absorptive cells, mucus-secreting cells, enteroendocrine cells, and Paneth cells. Compared with static monolayer cultures of Caco-2 cells, the differentiated 3D intestinal structures exhibit enhanced drug metabolism functions. Additionally, mechanical deformation induced by peristalsis has been shown to enhance the formation of 3D intestinal villi. These cells also exhibit the expression of tight junctions, the formation of brush borders, and mucus secretion. The GOC system is a reliable tool for drug screening, studying gut microbiota, investigating inflammatory factors, and examining the impact of peristalsis-induced mechanical deformation on intestinal diseases. This model not only simulates the complex physiological environment of the gut but also offers strong support for elucidating the mechanisms underlying gut health and disease.

The intestinal vascular network ensures that epithelial cells receive an adequate supply of oxygen and establishes an oxygen gradient within the gut lumen.[71] Most gut microbiota inhabit different locations based on their requirements for low-oxygen conditions. Given the crucial role of microbiota in human health, recreating these oxygen gradients and anaerobic environments *in vitro* is essential for a deeper understanding of their functions in both health and disease. Sasaki *et al.* developed a co-culture system featuring an integrated oxygen gradient.[72] In this system, human colon organoids can grow as a monolayer on Transwell membranes, which are then exposed to a hypoxic gas mixture and sealed with rubber stoppers. These methods provide an ample oxygen supply to the epithelial cells in the basal culture reservoir and enable the cultivation of anaerobic microbiota in the hypoxic apical chamber. By controlling the oxygen gradient, this system significantly advances the study of the gut *in vitro*.

2.2.2 3D structure simulation. The gastrointestinal tract exhibits significant structural and functional differences from the esophagus to the colon, each tailored to meet specific digestive and absorptive tasks. The esophagus consists of multilayered squamous epithelium, which primarily propels food from the mouth to the stomach *via* peristalsis, ensuring smooth entry into the digestive system.[73] The stomach lining, composed of a single layer of columnar epithelium, secretes gastric acid and digestive enzymes to assist in the initial stages of food digestion. The small intestine's inner surface is covered with villi and microvilli. These structures substantially increase the absorptive surface area, where enterocytes and goblet cells work synergistically to complete most nutrient absorption and mucus secretion.[74] The large intestine primar-

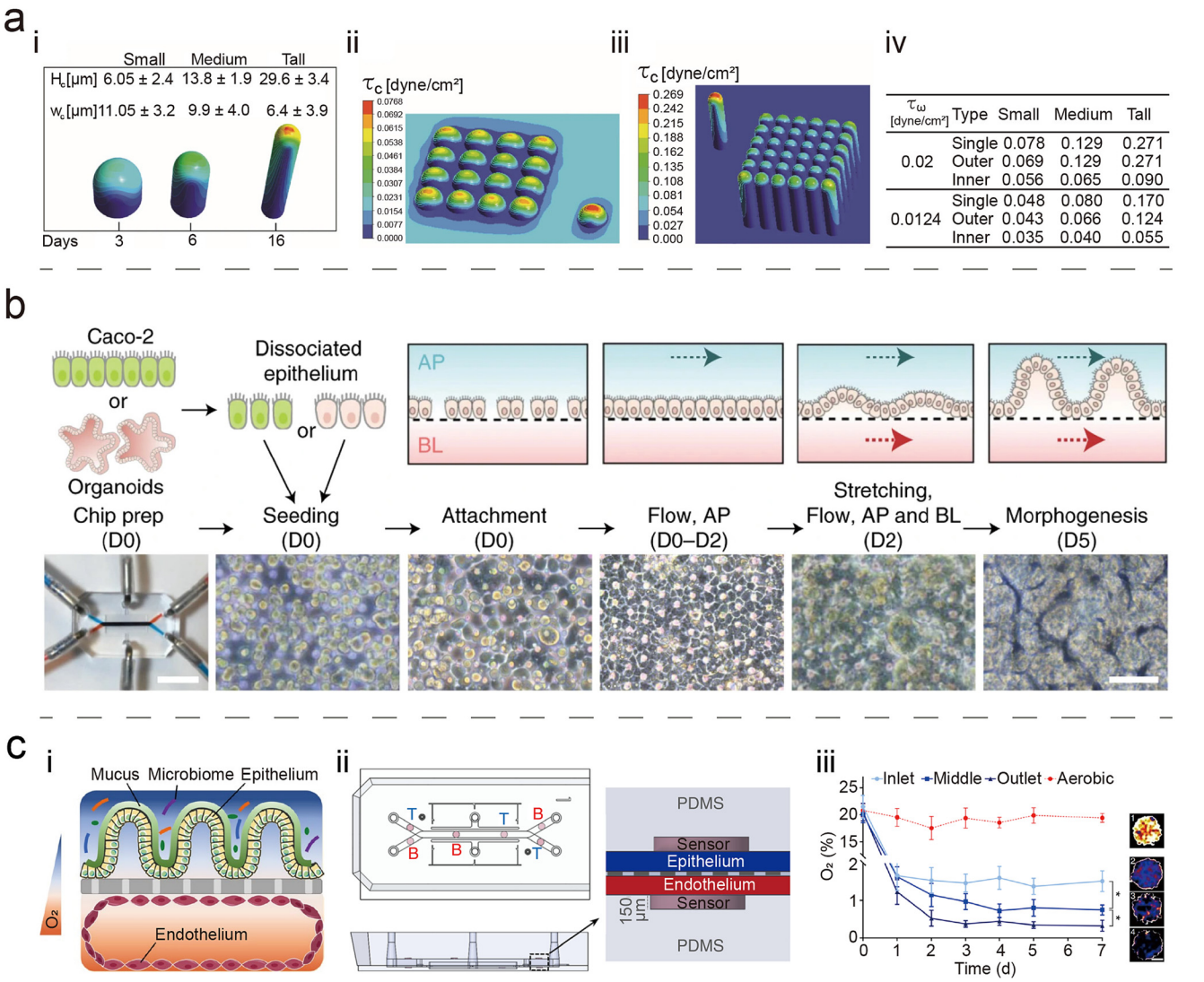

Fig. 2 Biomimetic gut model on microfluidic chip. (a) Fluid dynamics simulation of Caco-2 cells. (i) CFD simulations were performed on the geometric shapes and arrangements of three different types of cell. (ii and iii) In Ansys Fluent, CFD simulations were conducted for small cells (ii) and tall cells (iii) to predict their shear stress (τ_c) distribution. (iv) Based on the CFD simulation results, a summary of the predicted shear stress distribution was compiled. (Reprinted with permission from ref. 67. Copyright 2021, Springer Nature). (b) Induction of 3D intestinal morphology. After cell seeding and attachment to the PDMS porous membrane on day 0 (D0), apical (AP) flow was initiated immediately and maintained over the first two days (Flow, AP, D0–D2). Once a complete 2D monolayer had formed, basolateral (BL) flow was also introduced, accompanied by cyclic stretching (Stretch, Flow, AP, and BL). By D5 of microfluidic culture, the intestinal cells spontaneously entered the 3D morphogenesis phase (Morphogenesis, D5). (Reprinted with permission from ref. 68. Copyright 2022, Springer Nature). (c) An oxygen-sensing dual gradient GOC. (i) Schematic diagram of a two-channel microfluidic OOC device with an oxygen gradient. The system enables the co-cultivation of intestinal epithelial cells with aerobic and anaerobic bacteria, allowing for real-time oxygen concentration control. (ii) A schematic representation of the GOC. (iii) Oxygen concentration profiles in aerobically and anaerobically cultured GOC. (Reprinted with permission from ref. 69. Copyright 2019, Springer Nature).

ily reabsorbs water and electrolytes, while bacterial fermentation of undigested material leads to feces. The colon and rectum store and expel waste.[75] The different parts of the gastrointestinal tract work synergistically through their unique structures and functions, ensuring the efficient progression of digestion and absorption processes.

Oral medications must traverse the small intestine and be absorbed by the villi before entering the bloodstream. The villi play a crucial role in this process, making the study of intestinal villi essential for understanding drug absorption and gastrointestinal function. Current research often cultivates intestinal cells on flat surfaces to promote villus formation. However, Sung *et al.* achieved a breakthrough by developing a 3D hydrogel structure that accurately mimics the intestinal villi of the human gut.[76] The 3D structure comprises natural hydrogel material collagen and synthetic hydrogel material poly(ethylene glycol) diacrylate (PEG-DA). Collagen is the most abundant protein in mammals, widely distributed across various tissues.

As such, it has high biocompatibility, interacts well with intestinal tissues, and provides an ideal substrate for cell attachment and growth, which is crucial for simulating the extracellular environment of intestinal villi. PEG-DA hydrogel is transparent and highly hydrated, aiding in the recreation of the moist environment within the intestine while also facilitating the observation of cell growth and tissue formation processes. They processed natural and synthetic hydrogels into 3D geometries with high aspect ratios and curvature to replicate the structure of intestinal villi. Subsequently, they seeded the Caco-2 cell line onto these structures and cultured them, successfully generating finger-like projections resembling villi covered with epithelial cells. Similar to the study by Sung *et al.* in which a 3D hydrogel structure was successfully constructed, Shim *et al.* explored a 3D scaffold model simulating human intestinal villi.[77] However, they incorporated microfluidic technology with fluid shear stress, thereby enhancing the physiological relevance of the model. The team utilized photolithography to create a villus mold coated with alginate to form a soluble template. Collagen was cast onto the alginate, resulting in a scaffold with the desired patterned structure. They found that the 3D villus scaffolds generated stronger fluid shear stress, enhancing the metabolic function of Caco-2 cells. Under perfusion and 3D conditions, Caco-2 cells exhibited robust proliferation and formed an effective intestinal barrier. Shin *et al.* further simulated the physiological environment and biomechanical properties of the intestine by precisely controlling fluid flow and applying cyclic stretching (Fig. 2b).[68] The study successfully regenerated functional intestinal microstructures. Specifically, this approach utilized Caco-2 cells and organoid-derived intestinal epithelial cells to form a continuous 2D monolayer on the microfluidic platform. Basolateral flow and cyclic stretching were then applied to simulate the physiological functions and biomechanical environment of the intestine.

Other studies have also investigated the use of patterned scaffolds to facilitate the formation of villus-like structures. Wang *et al.* created micropatterns on the surface of polydimethylsiloxane (PDMS) substrates that closely mimic the dimensions of crypt structures found in natural tissues. These patterns were coated with fibronectin, and Caco-2 cells were seeded and cultured for up to 14 days.[78] The PDMS substrate provides a low-adhesion, biocompatible, breathable, and non-toxic surface for cells. Compared with the cell–matrix interactions in traditional 2D culture models, this cultivation condition promotes enhanced cell–cell interactions.[79] The results showed that Caco-2 cells cultured on patterned substrates exhibited higher mitochondrial activity and lower alkaline phosphatase activity in the early stages than cells grown on flat substrates. In contrast to the 2D cell culture model in Wang *et al.*'s study, the 3D model constructed by Chen *et al.* better recapitulates the physiological structure and function of the intestine.[80] This model utilizes a scaffold made of silk fibroin and PDMS materials, which enhances mechanical stability and promotes the diversified differentiation of cells. It successfully reconstructs multiple cell types of the intestinal epithelium, including enterocytes, goblet cells, and Paneth cells. Silk fibroin, with its excellent mechanical properties (high strength and good flexibility), significantly improves the scaffold's mechanical stability, enabling it to withstand pressures similar to those experienced by intestinal tissue *in vivo*. Moreover, the porous structure of the silk fibroin scaffold facilitates cell attachment, migration, and proliferation while also supporting the transport of nutrients and oxygen, as well as the removal of metabolic waste. This study demonstrates the feasibility of culturing human intestinal epithelial cells in a biocompatible 3D tubular silk scaffold system. The model closely simulates natural human infection processes, providing a valuable platform for studying interactions between mammalian cells, bacterial pathogens, and antibiotic resistance in acute and chronic contexts. These advancements significantly improve the *in vitro* reproduction of intestinal villous structures, further advancing research on gut function, drug absorption, and pathology.

2.2.3 Microbial environment simulation. In the previous discussion, we focused on the advancements in GOC models for simulating intestinal villus structures and fluid shear stress, which are crucial for intestinal absorption and barrier function. However, the physiological functions of the gut are not only dependent on the structure of its epithelial cells and mechanical stimulation but also closely related to the diversity and ecological balance of the gut microbiome. The gut microbiome, a complex ecosystem within the human body, plays an essential role in regulating immune functions, promoting digestion, and maintaining gut health.

The human intestinal microbiota, composed of diverse microorganisms, including bacteria, fungi, protozoa, viruses, and bacteriophages, forms a complex and dynamic ecosystem that maintains host intestinal function and overall health.[81] These microbes influence host physiology through metabolic regulation and immune modulation, and their dysbiosis has been closely linked to the onset and progression of various diseases. However, the mechanisms underlying host–microbiota interactions remain poorly understood. Conventional static culture models have significant limitations in advancing this field, as they fail to sustain long-term co-culture of intestinal cells with commensal microbiota. The rapid proliferation of bacteria often leads to contamination of the culture system, disrupting the experimental environment and compromising the results.[82] GOC technology, by precisely recapitulating the 3D architecture and dynamic microenvironment of the gut, overcomes many of these limitations, establishing itself as a transformative platform for investigating host–microbiota interactions. Marzorati *et al.* developed a host–microbiota interaction (HMI) microfluidic system to investigate the responses of Caco-2 cells to bacterial exposure.[83] The model consists of two chambers: one containing a mixed microbial community and the other housing intestinal cells. Their findings demonstrated that host and bacterial cells could survive for up to 48 hours in the HMI system. This study establishes the feasibility of microfluidic GOC systems for co-culturing cells with microorganisms, providing a valuable platform for further exploration of host–microbiota interactions. Kim *et al.*'s study incorporated the interaction between peripheral

blood mononuclear cells (PBMCs) and pathogenic bacteria, revealing the mechanisms of immune responses induced by bacteria and the resulting intestinal damage during the inflammatory process.[84] Researchers have used PBMCs to interact with lipopolysaccharide (LPS) or pathogenic *Escherichia coli* to explore intestinal inflammation. This interaction triggers a cascade of pro-inflammatory cytokines, including IL-8, IL-6, IL-1β, and tumor necrosis factor-α, disrupting the intestinal villus architecture and ultimately resulting in the loss of gut barrier function. The presence of PBMCs accelerates and exacerbates epithelial cell damage induced by pathogenic *Escherichia coli*. Additionally, the study investigates the role of probiotics in repairing intestinal injury.[82] For instance, when *Lactobacillus rhamnosus GG* was cultured on Caco-2 cell monolayers and compared with Transwell chambers, the bacterial microcolonies adhered tightly to the Caco-2 monolayers for 96 hours, enhancing gut barrier function. This demonstrates that probiotics can inhibit pathogen-induced villus damage, highlighting their potential application in maintaining gut health.

One particularly challenging aspect of modeling the microbiome is that most commensal microbes in the gut are anaerobic.[85] Therefore, creating an anaerobic environment is essential for understanding the role of gut microbiota in health and disease. Firoozinezhad *et al.* developed a microfluidic GOC system that successfully simulated the human body's interactions between the gut microbiome and intestinal epithelial cells (Fig. 2c).[69] This system established a physiologically relevant oxygen gradient, enabling the co-culture of intestinal epithelial and endothelial cells, and maintained anaerobic conditions for up to seven days. Experimental data demonstrated that, under anaerobic culture conditions, the gut barrier function was significantly enhanced compared with aerobic conditions, as indicated by a decrease in the permeability of intestinal epithelial cells (Papp value) from 3.1×10^{-7} cm s^{-1} to 1.6×10^{-7} cm s^{-1}. These findings suggest that anaerobic environments positively influence the stability of gut barrier function. Recent studies on the *in vitro* co-culture of intestinal cells and microorganisms are summarized in Table 1.

In summary, the GOC, which simulates the dynamic human intestinal microenvironment, offers distinct advantages over traditional gut models by more accurately recapitulating intestinal functions. This system not only integrates the complex gut microbiota but also facilitates the study of interactions between microbes and human intestinal epithelial cells, as well as the development of gut diseases. By reproducing the intricate physiological environment of the gut, the GOC demonstrates significant potential in basic research and provides new tools and methods for future drug screening, studies of host–microbe interactions, and personalized medicine.

3. Liver-on-a-chip

3.1 The design principles of liver biological structures

The liver, the largest internal organ, plays a central role in regulating systemic metabolism.[101] Its basic structural and functional unit is the liver lobule (Fig. 3a), which consists of hepatic acini. Each liver lobule features a hexagonal structure with a central vein at its core. At each vertex of the hexagon lies a portal triad, consisting of a hepatic artery, portal vein, and bile duct, while hepatocytes are arranged radially around the central vein.[102,103] These hepatocytes are organized into layers of uneven, plate-like structures known as hepatic plates. The spaces between adjacent hepatic plates are termed liver sinusoids (Fig. 3b), which are specialized capillaries composed of liver sinusoidal endothelial cells (LSECs) with an average diameter of 10 μm and a length of 275 μm.[104,105] The membrane of LSECs contains numerous open pores known as fenestrae, with diameters ranging from 100 to 1000 nanometers, resembling a sieve through which blood components can pass.[106,107] The region between the LSECs and hepatic plates is referred to as the sinusoidal space, a thin 1.4 μm-wide network of basement membranes composed of fibronectin, laminin, type IV collagen, and type I collagen.[108] Hepatocytes surrounding the liver sinusoids extend microvilli into this space, facilitating direct contact with the blood and increasing the effective surface area for interactions between hepatocytes and transported substances, thereby enhancing liver function. Additionally, hepatocytes exhibit polarity: adjacent cells form invaginations in their membranes that create small tubular structures known as bile canaliculi, which ultimately converge to form the common bile duct for bile excretion.[109] Moreover, the liver comprises parenchymal and non-parenchymal cells, with parenchymal cells accounting for approximately 60% of the total liver cell population.[110] These parenchymal cells are primarily responsible for the liver's fundamental physiological functions, including metabolism, detoxification, protein synthesis, and bile secretion. Hepatocytes, the main type of parenchymal cell, participate in various metabolic processes, such as the synthesis and breakdown of glucose, lipids, and proteins. Non-parenchymal cells include liver sinusoidal endothelial cells, Kupffer cells (KCs), and hepatic stellate cells (HSCs), which play essential roles in maintaining liver structure, regulating immune responses, and mediating cell-to-cell interactions within the liver.

Primary human hepatocytes (PHH) are widely regarded as the gold standard for *in vitro* liver cell culture models, as they can accurately reflect the specific metabolic functions and physiological activities of the human liver. However, the use of primary human hepatocytes is limited due to their scarcity and transportation difficulties, which restrict their application in large-scale experiments.[113] In contrast, hepatocyte cell lines, owing to their easy accessibility and high proliferative potential, are extensively used in *in vitro* studies. These cell lines are typically derived from liver tumor tissues or constructed through genetic engineering methods (such as HepaRG cells and HepG2 cells).[113] Although these cell lines differ from primary cells in terms of metabolic function and may experience a loss of differentiation status, their significance in standardized experiments, drug screening, and high-throughput testing remains indispensable.

Table 1 Summary of *in vitro* co-culture performance of intestinal cells and microbes

Cells	Microbes	Co-culture time	Performance	Ref.
Caco-2	*Shigella flexneri* 5a	2 days	The 3D villus-like structure is lost, and the height is reduced by about 75%	48
	B. fragilis	5–12 days	During the co-culture process, the intestinal barrier function was significantly enhanced, and the mucus layer secreted by intestinal epithelial cells formed a barrier between intestinal cells and microorganisms	69
	LGG	7 days	TEER increased by about 30%, and the co-culture model showed *an in vivo*-like microenvironment	82
	Escherichia coli	4 days	Intestinal barrier function and normal villus architecture were completely lost within 24–36 h	84
	Bifidobacterium adolescentis; *Eubacterium hallii*	7 days	TEER is improved by 20%, and the device is close to the chemical microenvironment of the human colon	86
	Lactiplantibacillus plantarum	5 days	This strain can inhibit the decrease in TEER value caused by LPS and increase TEER value in co-culture	87
Caco-2	Coxsackievirus B1	2 days	Villi could no longer be detected, which is indicative of a sudden complete loss of barrier function	88
	LGG; VSL#3	3 days	The intestinal epithelial layer destroyed by pro-inflammatory cytokines is transformed into a complete and restored mucosal morphology; it enhanced the localization of tight junction proteins, and elevated mucus production	89
	L. rhamnosus; *B. longum*	—	Prevents epithelial cell sloughing and loss of the brush border when the device is colonized with microorganisms, and increases TEER values	90
	VSL#3	—	VSL#3 increases intestinal barrier integrity disrupted by DSS treatment	91
	Blautia coccoides	2 days	In the presence of bacteria, epithelial cell activity was not reduced	92
	LGG; *B. caccae*	1 day	The cells exhibited tight junctions and dissolved oxygen concentrations comparable to human intestinal tissue	93
Caco-2; HUVECs	*L. rhamnosus*; *C. albicans*	1 day	*L. rhamnosus* colonization not only limits the growth of *C. albicans* but also reduces the translocation of the fungus over the intestinal barrier	94
	E. coli	2 days	COS reduced the coverage of *E. coli* on intestinal epithelial cells by 9.2%	95
	Lactobacillus casei	7 days	The coverage and height of the glycocalyx layer increased by 3% and 34%, respectively. After 7 days of co-culture, Caco-2 cells and *L. casei* were maintained above 97%	96
	SARS-CoV-2	5 days	Tight junctions identified by E-cadherin expression were severely disrupted, and the intestinal villus-like structure was damaged	97
	LGG; *E. coli*	1 day	ESBL-EC stimulation causes microstructure damage, mucus loss, and barrier function impairment.	98
Biopsy-derived organoids	*F. prausnitzii*; *Eubacterium rectale*; *B. thetaiotaomicron*	3 days	The intestinal epithelial barrier is intact and maintains its physical properties	99
	S. typhimurium; *E. faecium*	15 hours	Tight junctions were disrupted and mucus accumulation was reduced before lesions occurred	100

Lactobacillus rhamnosus GG (LGG), transendothelial electrical resistance (TEER), lipopolysaccharide (LPS), human umbilical vascular endothelial cells (HUVECs), VSL#3 (*L. paracasei*; *L. plantarum*; *L. acidophilus*; *Lactobacillus delbrueckii* subsp. Bulgaricus; *B. longum*; *B. breve*; *B. infantis*; *Streptococcus thermophilus*; *E. coli*), dextran sodium sulfate (DSS), chitosan oligosaccharides (COS).

In traditional 2D culture models, isolated primary hepatocytes often lose their differentiated structure and liver-specific functions.[114] However, when cultured in 3D models, isolated hepatocytes exhibit enhanced liver function *in vitro* and can maintain their differentiated characteristics longer.[115] Bioreactors have been proposed to better simulate the *in vivo* environment for developing *in vitro* 3D liver tissue models. Bioreactors are designed to precisely control the culture conditions of hepatocytes by regulating the nutrients and chemical composition of the culture medium, thereby optimizing cell growth and function.[116] Liver cell bioreactor cultures can be categorized into three main types: plate designs, packed bed designs, and hollow fiber designs.[117–119] Although these bioreactors facilitate the 3D culture of hepatocytes, challenges remain in accurately simulating the cellular microenvironment *in vitro*. These challenges include achieving precise control over the microenvironment and reproducing the complex cell–cell interactions *in vivo*.

Traditional *in vitro* simulation systems, while simple to operate and cost-effective, are typically static cultures that struggle to replicate the complex microstructures of liver tissue. Additionally, these systems often struggle to maintain cell viability for extended periods, typically not exceeding 2–3 days.[120,121] With advancements in micro–nano technology, significant progress has been made in developing *in vitro* liver models.[122] For example, the creation of micro-scale sub-microstructures that mimic the liver lobule architecture enables a more accurate reproduction of liver function within a physio-

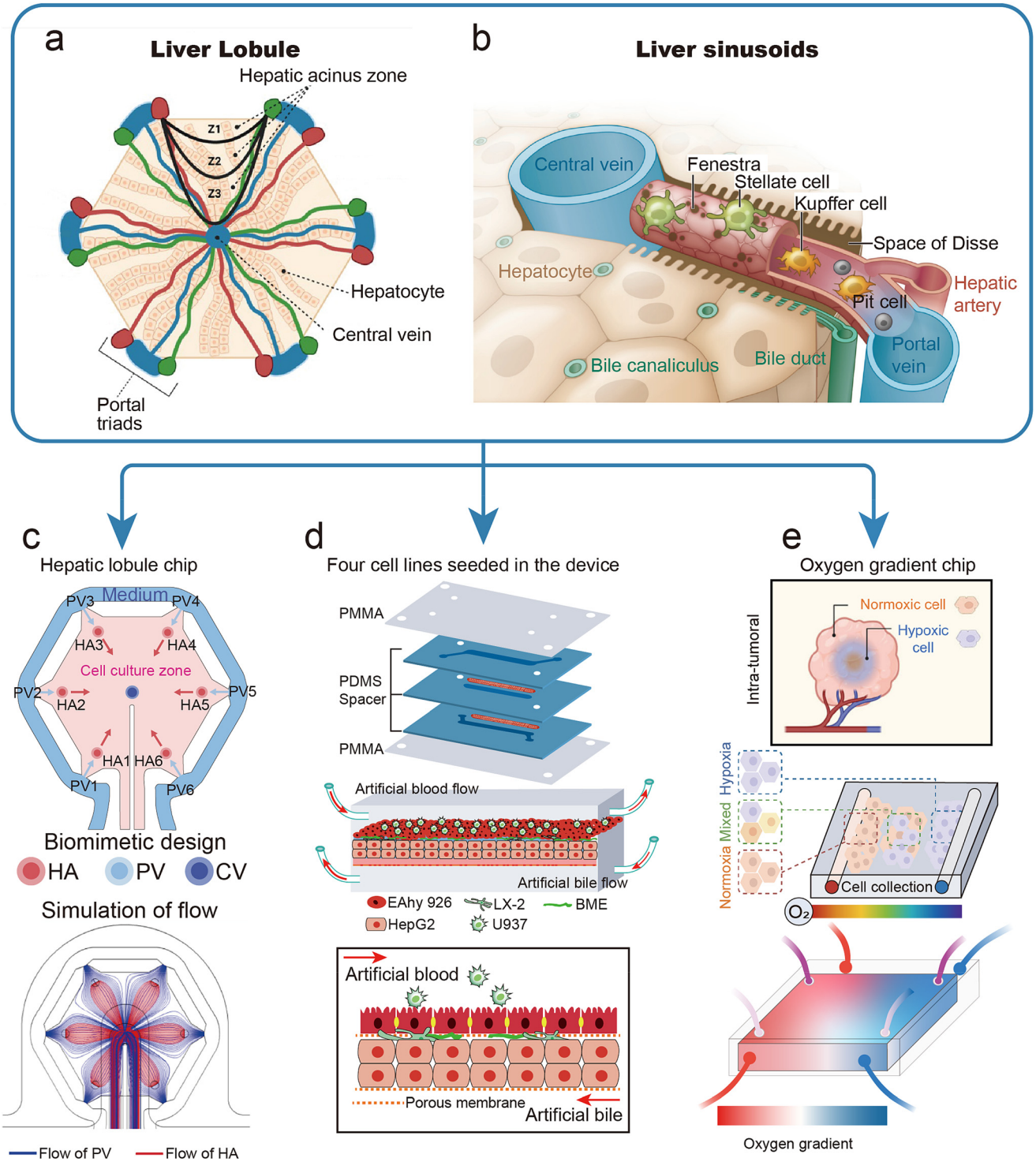

Fig. 3 Schematic representation of liver structure and LOC classification. (a) Schematic of a liver lobule. The liver lobule comprises hepatic acini, with zones Z1, Z2, and Z3 representing the hepatic acinar zonation. (Reprinted with permission from ref. 102. Copyright 2022, MDPI). (b) Schematic of the liver sinusoid. The liver sinusoid is a specialized capillary composed of fenestrated LSECs. (Reprinted with permission from ref. 105. Copyright 2019, Annual Reviews). (c) Biomimetic liver lobule chip (LC). This hexagonally designed chip features a central vein (CV), with the hepatic artery (HA) and portal vein (PV) positioned at the corners, providing a dual blood supply through both the portal vein and hepatic artery. (Reprinted with permission from ref. 111. Copyright 2021, Elsevier). (d) Schematic of the liver sinusoid on a chip. This device supports the co-culture of four different cell lines. (e) Schematic of the dual gradient chip. An oxygen gradient chip was developed to investigate the oxygen preferences of HCC and to cultivate HCC tissue fragments. (Reprinted with permission from ref. 112. Copyright 2019, Springer Nature).

logically relevant microenvironment (Fig. 3c).[111] These technologies provide a rapid, simple, and high-throughput approach, facilitating a more realistic replication of liver function.[123–125] In recent years, more advanced microfluidic platforms have been developed. These platforms can simulate the cellular microenvironment by controlling parameters such as cell–cell and cell–matrix interactions, shear stress, and metabolic products.[126–128] Combined with microfluidic technology, 3D dynamic liver cell models, called 'LOC', provide physiologically relevant culture conditions that better maintain cellular bioactivity.[129]

LOC represents a recent breakthrough in microphysiological systems, aiming to simulate the liver's anatomical structure and physiological functions through microfluidic technology.[110] As the primary organ responsible for metabolism and detoxification, the reconstruction of liver function is the core objective of LOC design. These chips typically integrate hepatocytes (parenchymal cells) and non-parenchymal cells (such as LSEC and KC) *via* 3D co-culture methods to achieve a high-fidelity simulation of the liver microenvironment.[130] One of the notable advantages of LOC is the incorporation of dynamic fluid systems. Shear stress not only maintains the polarization and activity of liver cells but also promotes the gradient distribution of oxygen and nutrients, further enhancing the metabolic capacity of the model.[131] Additionally, LOC allows for real-time monitoring of biomarker secretion, providing a potential means to assess liver function and drug responses dynamically.[132] Compared with traditional 2D culture systems and animal models, LOC exhibits significant advantages in simulating human-specific metabolism, particularly in predicting drug metabolites and toxicity responses with greater reliability. Their application spans a wide range, from metabolic and toxicity assessments in drug development to studying pathological mechanisms in chronic liver diseases, such as NAFLD and liver fibrosis, showing excellent prospects.[130] With ongoing advancements in chip design and biomaterials, LOC is expected to integrate more functional cell types and microenvironmental factors in the future, thereby providing a more comprehensive platform for precision medicine and personalized treatments.

Current LOC designs can be broadly categorized into several types. The first type is biomimetic microstructure design, which aims to replicate the structural organization of hepatocytes and their functional units on the chip. This includes establishing different concentration zones to simulate liver sinusoids and lobules *in vitro* and proportionally recreating liver structures by designing varied structural shapes and channel sizes.[133] The second type is co-culture systems, where different types of cell are incorporated into the culture to replicate the complex cellular composition found *in vivo* (Fig. 3d).[134] Co-culturing non-parenchymal cells, such as LAECs, KCs, HSCs, and lymphocytes with hepatocytes, is used to explore cell–cell and cell–matrix interactions. This approach enhances the physiological relevance of the model and allows for the investigation of cellular communication and the influence of the liver microenvironment on hepatocyte function.[135] The third approach entails simulating physiological parameters by manipulating factors such as shear stress resulting from fluid flow, mechanical stimulation, and oxygen gradients. This methodology aims to closely replicate the authentic physiological environment observed *in vivo* (Fig. 3e).[112] In the following sections, we will review the latest advances of microfluidic chip technology in the study of bionic liver structure and function, and delve into the limitations and challenges of existing research.

3.2 *In vitro* biomimetic liver structure and function on microfluidic chips

3.2.1 Structural simulation: liver sinusoids and liver lobules. Liver sinusoids are the essential functional units of the liver, composed of highly polarized microvascular endothelial cells with numerous fenestrae that facilitate the exchange of substances between the hepatocytes and the bloodstream. These sinusoids play a pivotal role in lipid metabolism, blood coagulation, cell growth, differentiation, immune responses, and inflammation. Reconstructing the microstructure of liver sinusoids *in vitro* is critical for liver research, as it allows for more accurate simulation of physiological functions and disease mechanisms.

In 2007, Lee *et al.* developed a bioinspired artificial liver sinusoid model, marking one of the pioneering efforts in creating microfluidic models for liver research.[133] They constructed the model using soft lithography techniques and successfully cultured primary rat and human hepatocytes, providing a functional *in vitro* platform to mimic liver sinusoid microenvironments. The model featured a dedicated cell chamber for hepatocyte seeding and a flow channel for circulating culture medium, nutrients, and drugs, separated by an endothelial barrier. This barrier effectively replicated the mass transfer properties of the hepatic acinus, restricting the direct flow of culture medium to the hepatocytes while facilitating the diffusion of essential nutrients and oxygen. However, the model primarily simulated the structure of the liver sinusoidal endothelial barrier and the diffusion of substances *in vitro*. It did not replicate more complex liver microstructures, such as the space of Disse, oxygen concentration gradients, or interactions with non-parenchymal cells. To address this challenge, Rennert *et al.* integrated a co-culture system comprising HUVECs, tissue macrophages, the human stellate cell line LX-2, and the hepatocellular carcinoma-derived cell line HepaRG to develop a more advanced liver layer.[136] This model features morphology akin to human liver sinusoids and effectively simulates the space of Disse by employing a suspended, freely perfusable membrane as the cell culture matrix.[137] Additionally, oxygen sensors were integrated at the inlet and outlet of the perfusion channels, facilitating the real-time measurement of cellular oxygen consumption. The model was able to maintain cell function *in vitro* for at least 4 days after being fully assembled and starting perfusion culture. Studies have demonstrated that hepatocytes exhibit significant differentiation and structural reorganization within this physiologically relevant environment, achieving polarization akin to that

of primary human liver tissue. This liver model represents a significant breakthrough in the *in vitro* simulation of liver function, offering a novel platform for studying hepatic physiology. Mi *et al.* also advanced the liver sinusoidal chip model by utilizing laminar flow technology and endothelial cell self-assembly techniques, successfully recreating the liver's fundamental functional unit—the liver sinusoid (Fig. 4a).[138] This study formed a dual-layer collagen structure with well-defined boundaries by injecting collagen gel containing HepG2 cells and HUVECs. The rat tail collagen type I used in the model, known for its high structural similarity to human collagen, demonstrated excellent biocompatibility, closely interacting with hepatic cells to promote adhesion, growth, and functional expression.[139] Furthermore, its degradable properties align with the natural turnover of the hepatic extracellular matrix, which is crucial for maintaining the long-term stability and functionality of the liver model. By precisely regulating the density of HUVECs and the injection of growth factors, the researchers successfully induced the self-assembly of HUVECs into a monolayer structure within the collagen matrix, effectively mimicking the sinusoidal endothelial layer. Experimental results showed that the model maintained high cell viability and stable liver functions, such as albumin secretion and urea synthesis, for at least seven days. This study offers a novel approach to constructing high-fidelity, long-term, stable *in vitro* liver sinusoid models, holding great potential for advancing liver physiology and pathology research.

In addition to replicating the liver sinusoid, liver lobules—constituting the main component of the liver—exhibit a diverse array of dynamic physicochemical signals and microenvironmental structures. To enhance our understanding of the structural characteristics and interactions of cells and tissues, simulating liver lobules *in vitro* is particularly essential. Ho *et al.* designed a star-shaped electrode array utilizing a dual-electrophoresis method to reconstruct a pseudo-hexagonal model that represents liver lobules, effectively mimicking the classic morphology of liver lobules.[103] In this model, HepG2 cells and HUVECs were guided and arranged by an electric field to form a liver lobule-like structure. After dielectrophoretic cell patterning, the research team assessed cell viability through staining, revealing a high cell survival rate of 95%. Further experiments demonstrated that after two days of co-culture, the combination of HepG2 cells and HUVECs significantly enhanced cytochrome P450 (CYP450) enzyme activity, with an increase of up to 80%. Banaeiyan *et al.* developed a large-scale liver lobule chip design that warrants attention.[143] This model consists of hexagonal tissue culture chambers for culturing HepG2 cells and hiPSC-derived hepatocytes. Each chamber features a central outlet that simulates the central vein of the liver lobules. In contrast, isolation chamber walls separate the culture chambers from the channels, protecting the cells from convective shear stress while allowing nutrient diffusion. This model effectively simulates liver lobule, sinusoid, and portal vein structures at physiological scales, demonstrating stable albumin secretion, urea synthesis, and the formation of bile canaliculus networks. This platform holds significant promise for future applications in co-culture studies and drug-induced hepatotoxicity research. Although the lobule chip developed by Ban *et al.* demonstrates significant advantages in mimicking liver structure and function, the need for more precise control over the cellular arrangement and microenvironment remains unmet. Chen *et al.* developed a lab-on-a-chip that simulates liver lobules, comprising three main components: a concentration gradient generator, a dielectrophoretic cell patterning system, and four cell culture chambers that create a microenvironment conducive to cell cultivation (Fig. 4b).[140] This study successfully patterned C3A cells (human hepatocytes) and NIH/3T3 cells (fibroblasts) within a GelMA-based microenvironment. GelMA, a hydrogel with biocompatibility and photopolymerizable properties, provides a 3D culture environment resembling the liver's natural ECM, crucial for maintaining hepatocyte morphology and function. In the experiment, GelMA hydrogel was applied over cell patterns on a microfluidic chip, effectively shielding the cells from shear stress while ensuring a stable nutrient supply, thereby supporting long-term functional and structural stability. This technique successfully replicated the cellular arrangement characteristic of liver lobules. Furthermore, experimental results demonstrated that cell viability was significantly enhanced in a 5% GelMA hydrogel environment, and urea secretion reached its highest levels, underscoring the critical role of an optimal hydrogel microenvironment in maintaining cell organization and enhancing liver function. By precisely controlling cell patterning and physiological conditions, this chip offers a novel platform for studying hepatocyte interactions and liver-specific functions, presenting significant potential for biomedical applications. Subsequently, Cottier *et al.* developed a primary hepatocyte micro-patterned co-culture (MPCC) model to replicate the pathological processes of hepatic steatosis and NAFLD.[144] The study demonstrated that exposure to free fatty acids (FFA), high glucose and fructose, or their combination effectively induced steatosis. Additionally, the therapeutic potential of ACC1/ACC2 inhibitors in preventing and reversing steatosis was validated. The model also successfully evaluated valproic acid-induced drug-related steatosis and detected significant changes in gene expression associated with NAFLD. In another study, Ware *et al.* demonstrated that the micro-patterned co-culture of HepaRG cells with mouse embryonic 3T3-J2 fibroblasts significantly enhanced hepatocyte functionality and improved the practicality of drug screening.[145] The research showed that co-culture model substantially increased albumin secretion, maintained more stable cytochrome P450 activity, and improved both the sensitivity and specificity of predicting drug-induced liver injury. These findings underscore the broad potential of the MPCC system in drug metabolism and pharmacokinetics research.

Although the simulation of liver sinusoids and liver lobules has yielded promising results and found widespread application in liver tissue engineering, the aspiration to develop *in vitro* liver microtissues with a complete ultrastructure remains unrealized. To create more comprehensive *in vivo*-like

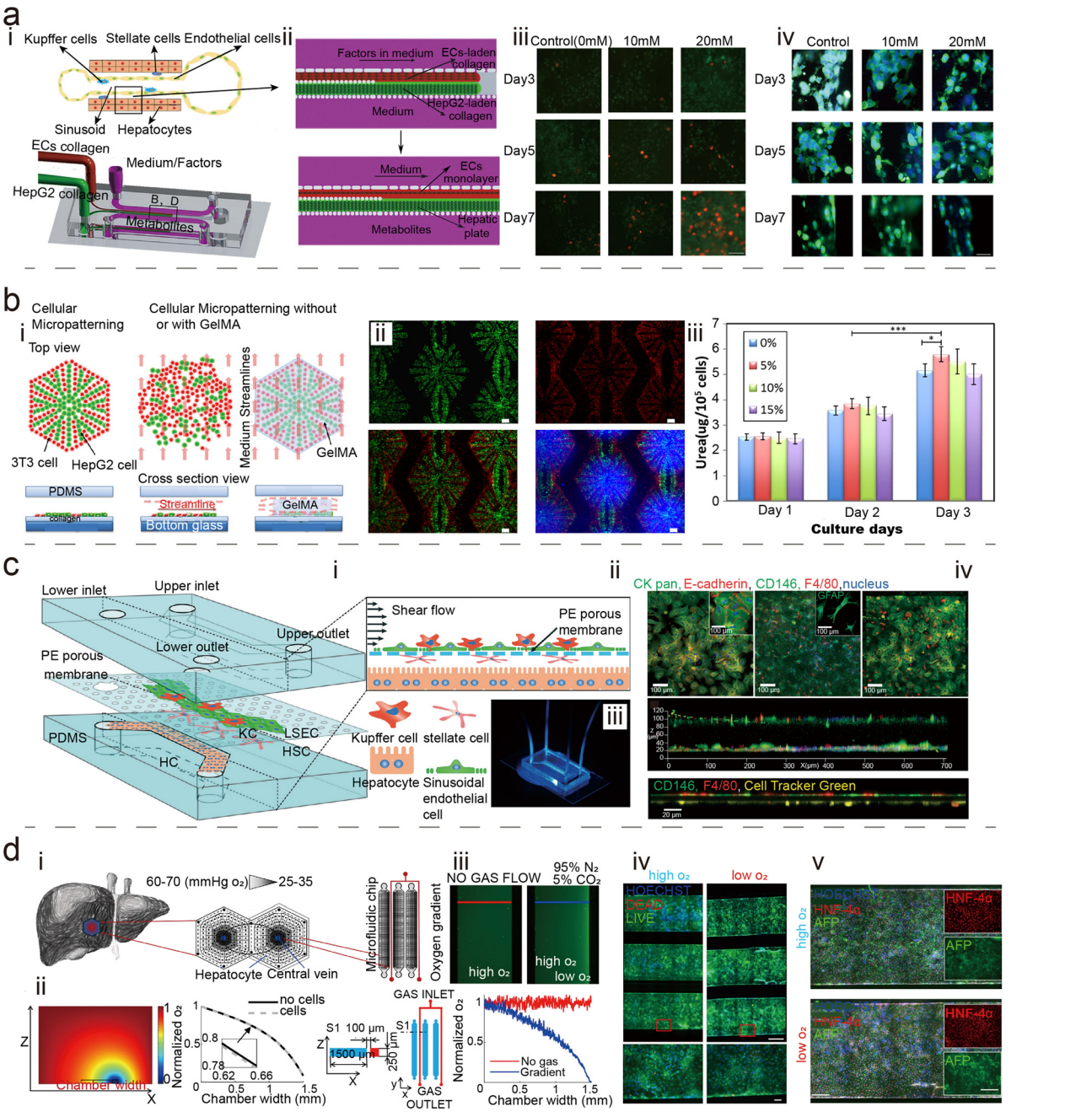

Fig. 4 Biomimetic liver model on a microfluidic chip. (a) Liver sinusoid on a chip. (i and ii) Formation of the biomimetic liver sinusoid on a chip. This chip simulates the liver sinusoid, primarily composed of hepatic plates and a monolayer of endothelial cells. Collagen, loaded with HepG2 cells and HUVECs, is synchronously injected into the central chamber at a controlled flow rate. (iii) Live/dead images at different acetaminophen (APAP) concentrations. (iv) Immunofluorescence images of albumin with different APAP concentrations. Scale bar: 50 μm. (Reprinted with permission from ref. 138. Copyright 2018, IOP Publishing). (b) Liver lobule simulation chip. (i) This chip replicates the morphology of liver lobules and incorporates a biocompatible, photocrosslinked hydrogel-based microenvironment to sustain cell patterns and functions. (ii) Patterning of C3A and NIH/3T3 cells. (iii) Urea secretion at varying concentrations in GelMA microenvironments post 3-day culture. Scale bar: 100 μm. (Reprinted with permission from ref. 140. Copyright 2021, Elsevier). (c) 3D liver sinusoid on a chip. (i) Microfluidic structure. This chip consists of two PDMS chambers, each measuring 100 μm in height and 1 mm in width, separated by a 10 μm-thick polyethylene membrane with 0.4 μm diameter pores. (ii) 3D assembling. (iii) Photographic image of an *in vitro* 3D liver sinusoid. (iv) 3D liver sinusoidal chip for identifying 4 mouse hepatocyte cell lines *in vitro*. (Reprinted with permission from ref. 141. Copyright 2017, Royal Society of Chemistry). (d) Oxygen gradient validation in LOC. (i) Hepatocytes naturally experience an oxygen gradient along the portal–central axis, differentiating "periportal" hepatocytes from "perivenous" hepatocytes. (ii) Simulation of steady-state oxygen concentration in the vertical cross-section of a PDMS chip. (iii) Fluorescence images of the culture chamber. (iv) Live/dead assay showing high (left) and low (right) O_2 differentiated hESCs at day 12 in microfluidic chips. (v) Day 13 differentiated hESCs showing HNF-4α (red) and alpha-fetoprotein (green). (iv) Scale bars 300 μm (microchannels, above) and 10 μm (enlargement, below). (v) Scale bars 100 μm (microchannel) and 50 μm (inset). (Reprinted with permission from ref. 142. Copyright 2019, Springer Nature).

structures, it is essential to integrate biological and engineering approaches, ensuring the provision of the requisite chemical and mechanical conditions to establish these specific architectures.[146,147]

3.2.2 Reproducible multicellular culture *in vitro*. Although current *in vitro* models of hepatic sinusoids and liver lobules have made significant progress in simulating the liver microenvironment and recreating the basic functions of liver cells, they still have certain limitations. Specifically, non-parenchymal cells in the liver, such as Kupffer cells, stellate cells, and sinusoidal endothelial cells, play a crucial role in maintaining liver cell function and regulating liver physiological responses. However, the intricate interactions between these cells, especially their roles in drug metabolism and inflammatory responses, have not been fully represented in existing *in vitro* models. To address these issues, researchers are introducing more non-parenchymal cell populations and, through refined fluid dynamics design, further exploring how to reconstruct a system *in vitro* that more closely resembles the *in vivo* liver microenvironment.

The development of *in vitro* liver sinusoid and liver lobule models is inspired by their *in vivo* morphological structures. Although these models can simulate the diffusion channels of the endothelial layer, these non-biological endothelial-like barriers replicate only the structural aspects of the *in vivo* liver microenvironment. They do not adequately reproduce living organisms' complex cellular interactions and drug metabolism processes. According to liver physiology, non-parenchymal cell populations support hepatocyte function and modulate inflammation.[105] For instance, KCs are responsible for clearing senescent red blood cells, bacteria, and various endogenous toxins; hepatic stellate cells store vitamin A and regulate blood sinusoid perfusion; and LSECs protect hepatocytes from toxic damage by secreting growth factors such as hepatocyte growth factor (HGF and interleukin-6).[148–150] Table 2 presents the constituent cells of the liver. The complexity of *in vivo* organs poses significant challenges in fully replicating them *in vitro*, particularly regarding manipulating cell–cell interactions outside the body.[151,152] Maher *et al.* developed a simple microfluidic dual-layer device that preserves primary human hepatocyte phenotypes in a static culture medium using a straightforward single-culture format.[153] In their experiments, the researchers introduced primary human hepatocytes alongside human LAECs. After co-cultivation, the hepatocytes displayed a cuboidal morphology and formed bile canaliculi networks, indicating that they can sustain robust functionality within this environment. The device features a flexible structure incorporating various non-parenchymal cell types, enabling co-cultivation effects. This makes it a preliminary model for investigating cell–cell interactions *in vitro*. However, the model lacks a dynamic physiological environment and cannot effectively replicate the liver microenvironment *in vitro*. Consequently, while this device provides certain advantages for studying cell–cell interactions, further development of complex models with dynamic physiological parameters is essential to simulate the intricate *in vivo* liver microenvironment fully.

In a study by Prodanov *et al.*, primary human hepatocytes were co-cultured with endothelial cells (EA.hy926), stellate cells (LX-2), and Kupffer cells (U937) within a microfluidic chip.[154] The chip features two microfluidic chambers separated by a porous membrane, with cells seeded to replicate the liver microenvironment found in the human body. ECs and KCs were seeded on the upper side of the membrane, while stellate cells were combined with a collagen solution and positioned beneath the membrane to simulate the space of Disse. Hepatocytes were seeded at the bottom of the lower chamber. The porous membrane simulated the fenestrated structure of liver sinusoids, protecting the hepatocytes from direct fluid shear stress while allowing for the exchange of culture medium and oxygen through diffusion, closely resembling *in vivo* conditions. This design not only replicates the 3D architecture of the liver but also simulates its microenvironment through dynamic fluid flow. The study confirmed that the reconstituted liver sinusoid microstructure model can be successfully maintained for 28 days. Compared with static cultures, albumin synthesis and urea excretion were significantly enhanced under dynamic flow conditions, while changes in CYP450 metabolic activity remained minimal. In 2017, Du *et al.* successfully developed an *in vitro* 3D liver sinusoid chip that integrates four primary murine liver cell types to replicate the key structures and functions of the liver sinusoid (Fig. 4c).[141] The research team used immunofluorescence staining to confirm that hepatocytes (HCs) were densely packed in the lower layer of the chip, expressing E-cadherin and CK pan markers. Meanwhile, LSECs and KCs formed a monolayer in the upper channel, marked by CD146 and F4/80, respectively, while HSCs were positioned on the basal side without specific staining to maintain background clarity. Under physiological microenvironmental conditions and fluid shear stress, this model demonstrated enhanced liver-specific functions, including albumin secretion, HGF production, CYP450 metabolic activity, and neutrophil recruitment responses. This work provides an innovative *in vitro* platform for studying intercellular interactions and immune responses in the liver.

Deng *et al.* recently developed a more sophisticated perfusion system based on a PDMS sandwich structure featuring porous membranes.[155] The system comprises three microfluidic chambers—upper, middle, and lower—sequentially accommodating four types of human-derived cell (HepG2, LX-2, EA.hy926, and U937) based on their physiological distribution.

Table 2 Characteristics of liver cells

Cell type	Diameter (μm)	Density (g mL^{-1})	Volume (% total)	Number (% total)
Hepatocytes	20–30 μm	1.07	70–85%	60–70%
Kupffer cells	10–15 μm	1.077	2–3%	5–15%
Stellate cells	7–10 μm	1.05	1.4%	5–8%
Sinusoidal	5–8 μm	1.03	2–3%	15–20%

Additionally, the system incorporates artificial hepatic blood flow and bile flow to more accurately simulate the complex medium flow environment of liver sinusoids. The study evaluated the hepatotoxicity of acetaminophen and assessed the alterations in acetaminophen-induced hepatotoxicity when combined with adjunctive medications. The results demonstrate that the device exhibits strong synthesis and secretion functions and enhanced cytochrome P450 enzyme activity, providing a more precise hepatotoxicity assessment than primary liver cell plate models. In the future, this innovative *in vitro* model could serve as a functional platform for investigating the maintenance of liver sinusoid functions, cell–cell communication, toxic metabolism, and inflammatory cascades. This advancement offers a more precise and effective tool for drug testing and disease research, significantly advancing the development of liver *in vitro* models.

3.2.3 Physiological parameter simulation: oxygen, shear stress. Despite successfully reproducing liver cell model structures and intercellular interactions in previous studies, constructing a comprehensive, functional *in vitro* platform that accurately mimics the liver microenvironment remains a significant challenge. In addition to the reconstruction of cell types and tissue architecture, dynamic physiological parameters within *in vitro* models are equally critical. The physiological functions of the liver are not solely dependent on cellular and tissue morphology but are also influenced by factors such as oxygen levels and shear stress. These physiological parameters are intricately regulated *in vivo* through blood flow, gas exchange, and intercellular signaling, supporting the liver's metabolism, differentiation, and functional maintenance. Consequently, one of the key challenges in replicating the liver microenvironment *in vitro* is the accurate reconstruction of these dynamic physiological conditions, particularly the gradients of oxygen concentration and shear stress.

The *in vivo* microenvironment of the liver is highly complex. When constructing *in vitro* liver cell models, it is essential to consider the tissue structure, cell–cell interactions, and various dynamic physiological parameters. Oxygen is critical in the liver microenvironment, significantly influencing cellular metabolism, differentiation, and growth.[118,156] *In vivo*, the liver receives oxygen from the portal vein circulation and maintains adequate oxygen levels through high-oxygen arterial circulation.[157] Existing static *in vitro* cultures acquire oxygen through air–liquid interface diffusion, whereas dynamic cultures depend on the oxygen present in the perfusion medium. An oxygen concentration gradient exists along the liver sinusoid, extending from the portal vein to the central vein. This gradient significantly influences gene expression and hepatocyte metabolism, forming functional zones within the liver.[158] Kang *et al.* developed a microfluidic platform termed "Metabolic Patterning on a Chip" (MPOC), which actively generates a range of oxygen concentrations, from normoxia to severe hypoxia, across a single continuous micro-tissue.[159] They exposed primary rat liver cells to an oxygen gradient ranging from 0.3% to 6.9% and observed that increasing hypoxia decreased cell viability by approximately 80%. This finding indicates that hepatocytes exhibit distinct metabolic and genetic responses to varying oxygen levels. This oxygen gradient platform can be adapted to study other hypoxic tissues, such as tumors, and to investigate drug toxicity and efficacy under hypoxic conditions. Tonon *et al.* expanded on applying oxygen gradients in cellular differentiation by precisely controlling oxygen levels to guide the differentiation of human embryonic stem cells into metabolically distinct hepatocyte subtypes (Fig. 4d).[142] This microfluidic chip design generated a stable oxygen gradient, ranging from high oxygen levels (160 mmHg, approximately 21%) to low levels (15 mmHg, approximately 2%). On day 12 of differentiation, cells cultured under high and low oxygen conditions exhibited high viability and minimal cell death. By day 13, cells were uniformly expressing hepatocyte nuclear factor 4α (HNF-4α) and α-fetoprotein under varying oxygen conditions. These findings demonstrate that an oxygen gradient is essential for maintaining hepatocyte differentiation potential and survival.

In addition to oxygen, shear stress is a crucial physiological parameter when designing perfusion-based LOC systems. The fluid's viscosity generates shear stress within the chip's channels, and its variation is closely linked to both the flow rate of the medium and the medium's viscosity. According to the research by Tilles *et al.*, exposure to shear rates exceeding 5 dyn cm^{-2} (0.5 Pa) significantly diminishes liver cell function.[118] Similarly, experimental results by Tanaka *et al.* demonstrated that low shear stress flow conditions lead to an increased rate of albumin synthesis.[160] To address the challenge of shear stress, it is essential to strike a balance between the shear stress induced by media flow and the oxygen content within the culture environment. A common approach involves selecting lower media flow rates while increasing the oxygen concentration within the chip or limiting the density of the hepatocytes, ensuring that the cells receive an adequate supply of oxygen.[161,162] Additionally, incorporating porous membranes or diffusion channels into chip designs can help isolate media flow, thereby protecting the cells from shear stress.[126] By optimizing these parameters, it is possible to more accurately replicate the liver's *in vivo* microenvironment, thereby enhancing the functionality and stability of *in vitro* hepatic models. This advancement provides a more reliable platform for drug testing and disease research.

4. Gut–liver-on-a-chip

4.1 Interaction in gut–liver-on-a-chip

In the human body, organs interact in several critical ways. (1) They maintain specific environmental boundaries through their structure and function integrity, ensuring tissue homeostasis and proper organ function. (2) Vascular endothelial cells form an endothelial barrier that isolates blood from tissues, regulating the dynamic exchange of blood components and cells across various tissues. (3) The circulatory system functions as a communication network among organs, facilitating the exchange of substances and the transmission of signals

through blood flow, thereby enhancing intercellular communication. These mechanisms are essential for maintaining tissue homeostasis and regulating the dynamic balance between health and disease.

The integration of multi-organ tissue systems enables the simulation of complex organ–organ interactions, offering critical insights for pharmacokinetics and pharmacodynamics (PK/PD), physiologically based pharmacokinetic (PBPK) modeling, ADME (Absorption, Distribution, Metabolism, and Excretion) analysis, quantitative systems pharmacology (QSP), and various computational modeling approaches.[163] Currently, a variety of systems have been developed to investigate multi-organ interactions. Kang *et al.* developed a gut–liver axis chip to investigate the effects of microbiome-derived metabolites and extracellular vesicles on hepatic cell function.[164] The results demonstrated that these microbiome-derived substances significantly enhanced albumin and urea secretion in HepG2 spheroids, suggesting a potential role of the microbiome in regulating liver function. This chip provides an effective platform for studying the interactions between the gut microbiome and host cells, particularly in the context of liver metabolic function. In studying the gut–liver axis, applying microfluidic technology and a multi-organ co-culture platform provides a new perspective for understanding the complex interactions between the gut and other organs. The four-organ chip system developed by Maschmeyer *et al.* expands this research perspective (Fig. 5a).[165] This system simulates the interactions between the intestine, liver, skin, and kidneys, utilizing microfluidic channels and micropumps to replicate the physiological circulation, thereby ensuring the exchange of substances and metabolic balance between the different tissues. In this setup, intestinal tissue developed villus-like 3D structures up to 270 μm and expressed cytokeratin 19 (Ctk 19) along the crypt–villus axis, demonstrating physiological polarization. Liver tissue maintained CYP3A4 expression, confirming its metabolic function. Skin biopsy samples cultured at the air–liquid interface formed a stratified stratum corneum, retaining proliferation and differentiation functions as evidenced by Ctk 10 and Ctk 15 expression. The proximal tubule cells of the kidney layer sustained basolateral Na-K-ATPase expression throughout the 28-day co-culture, indicating their transport functionality. These findings suggest that this four-organ-on-a-chip system effectively simulates human ADME (Absorption, Distribution, Metabolism, and Excretion) processes, providing a promising *in vitro* drug development and toxicity testing model. Li *et al.* proposed a novel system in which Caco-2 cells (simulating the gut) and rat primary glomerular endothelial cells (representing the kidneys) are co-cultured within segregated microchambers of a microfluidic device.[166] Using digoxin as a model drug, the system investigates the impact of intestinal drug absorption on renal toxicity *in vitro*, yielding results that align with clinical observations. Jeon *et al.* developed a microfluidic GLOC that reproduces the absorption of fatty acids in the gut and the subsequent lipid accumulation in hepatocytes (Fig. 5b).[167] In this study, varying concentrations of palmitic acid (PA) were applied to HepG2 liver cells to observe PA-induced oxidative stress responses. HepG2 cells cultured in standard plates exhibited a concentration-dependent response, with fluorescence signal intensities increasing by 3.06%, 8.99%, and 23.21% for respective PA concentrations. In contrast, cells co-cultured in a gut–liver chip under static conditions showed a weaker response, with fluorescence increases of 2.20%, 4.40%, and 8.33%. However, when the flow was introduced within the chip, the fluorescence intensities increased significantly to 1.48%, 3.86%, and 13.00% for 0.4 mM, 0.8 mM, and 1.2 mM PA, respectively. These data suggest that flow conditions, which mimic intestinal peristalsis, reduce the thickness of the unstirred water layer, thereby enhancing PA absorption and the oxidative stress response, particularly under 1.2 mM PA treatment where flow notably amplified oxidative stress. This suggests that the GLOC can partially replicate the dynamic interactions of drugs in the gut and liver, thereby enhancing the predictability of drug efficacy.

A significant example of organ interaction in the human body is first-pass metabolism, where drugs undergo intricate absorption and metabolic processes in the gut and liver. This involves simultaneous transport and reactions occurring at multiple locations within these organs. However, conventional *in vitro* cell culture models often struggle to replicate this process accurately. To address this challenge, Midwoud *et al.* developed a microfluidic-based system specifically designed for metabolic studies.[169] The system utilizes a two-chamber co-culture perfusion system with continuous medium flow to perfuse intestinal and liver tissue slices sequentially. The results indicate that intestinal and liver tissue slices maintain viable metabolic rates for at least 8 hours and 24 hours, respectively, demonstrating the system's suitability for intestinal and hepatic metabolism studies. Chen *et al.* developed an innovative microfluidic GLOC model to replicate first-pass metabolism accurately.[170] The chip features two adjacent, independent layers comprising intestinal epithelial cells (Caco-2) and liver cancer cells (HepG2). Drugs enter the liver chamber from the intestinal chamber, effectively replicating the processes of absorption and metabolism. During co-culture, the physiological functions of both cell types were observed to undergo alterations. Cytochrome P450 metabolic activity was significantly enhanced, and the absorption characteristics of Caco-2 cells were altered under flow conditions. This indicates that the co-culture system enhances the physiological relevance of the *in vitro* model. Subsequently, the team successfully simulated the absorption of fatty acids through the intestinal layer and their deposition within hepatocytes.[171] Tsamandouras *et al.* developed a novel fluidic platform that interconnects multiple organ models for pharmacokinetic research.[172] Studies of gut–liver cell co-cultures found that organ interactions can enhance hepatic metabolism. They also investigated the interactions between gut and liver tissues under both normal and inflammatory conditions.[173] The results revealed that interactions between the gut and liver in an inflammatory environment exacerbate the inflammatory response, negatively affecting tissue function. This under-

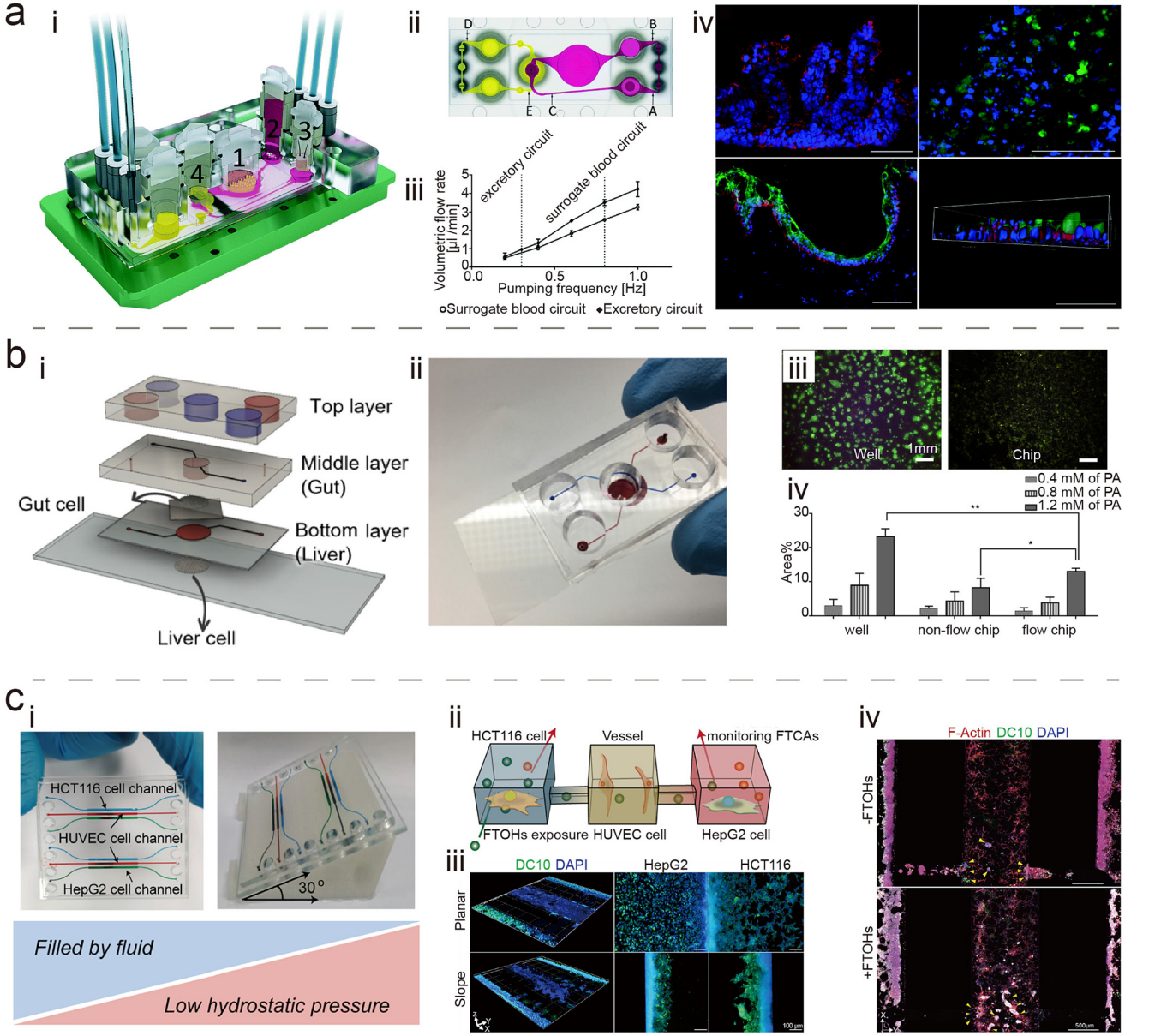

Fig. 5 Gut–liver co-culture on chips. (a) MOC with four types of co-cultured cell. (i) The device consists of two polycarbonate covers and a PDMS glass chip, featuring an alternative blood circuit (pink) and excretion circuit (yellow). (ii) Evaluating fluid dynamics in a device using μPIV. (iii) Pumping frequency and volume flow rate relationship diagram. (iv) Effect of 28-day coculture of human tissue in the device. Bars = 100 μm. (Reprinted with permission from ref. 165. Copyright 2015, Royal Society of Chemistry). (b) Microfluidic GLOC. (i and ii) The chip comprises three PDMS layers, with gut and hepatocytes positioned along the border of a polyester membrane. (iii) DCF-DA staining fluorescence micrograph after PA treatment. (iv) Fluorescence intensity analysis under different culture conditions. (Reprinted with permission from ref. 167. Copyright 2021, John Wiley and Sons). (c) Microfluidic-based gut–vascular–endothelium–liver co-culture chip. (i) This chip features a 3D gel scaffold with channels for venous endothelial cells, intestinal epithelial cells, and hepatic epithelial cells. (ii) Schematic diagram of connection design between channels. (iii) Confocal images of HepG2 and HCT116 cultured under flat or slope conditions. (iv) Immunofluorescence of DC10 and F-actin after FTOH treatment. (Reprinted with permission from ref. 168. Copyright 2023, American Chemical Society).

scores the significance of multi-organ platforms in understanding complex pathophysiological processes.

Bricks *et al.* employed a distinct biological model to simulate interactions between the gut and liver.[174] They conducted dynamic co-cultures of gut cells (Caco-2 TC7) and hepatocytes (HepG2 C3A) using a bioreactor to track the transport of phenacetin across the intestinal barrier. Compared with static culture dishes, their bioreactor demonstrated increased metabolic activity. Milani *et al.* utilized a GLOC system, co-culturing Caco-2 cells with HT29 cells in the gut chamber alongside primary human hepatocytes in the liver chamber.[175] In this study, HT29 cells, a human colon adenocarcinoma cell line,

are widely used to simulate the biological behaviors of intestinal epithelial cells. Their proliferative capacity allows a more precise representation of intestinal–liver interactions within OOC systems. Through this gut–liver co-culture model, the researchers effectively assessed the clearance rates and permeability parameters of prodrugs, active drugs, and glucuronide metabolites, further elucidating the critical role of intestinal metabolism in the MPA glucuronidation process. Moreover, the results were consistent with *in vivo* data. Lucchetti *et al.* developed an integrated GLOC platform to model drug metabolism along the gut–liver axis.[26] This platform combines the human–microbial crosstalk GOC with the Dynamic42 LOC, maintaining the viability and function of both intestinal and hepatic cells and successfully replicating the metabolism of the colorectal cancer drug irinotecan. The study further revealed that *Escherichia coli* can convert the inactive irinotecan metabolite SN-38G into the toxic metabolite SN-38, impacting drug metabolism. These findings offer new perspectives on how gut microbiota can influence drug response, presenting potential strategies for drug development. Additionally, they applied the GLOC to study the pharmacokinetics of mycophenolate mofetil and its two major metabolites, demonstrating the potential of this system to explore how intestinal and liver processes jointly determine the exposure of prodrugs and their metabolites. Other models investigating the gut–liver relationship have also been developed, including those focused on nanoparticle-induced damage and the toxic effects of PM2.5.[176,177] These approaches, which integrate multicellular tissue structures, multiple microphysiological systems (MPS), and quantitative mechanistic modeling, have been widely applied in preclinical drug development, emerging as powerful research tools.

While current gastrointestinal–liver systems are primarily employed to study metabolism and inter-organ communication, they do not fully replicate the enzymatic digestion process. To address this issue, Haan *et al.* developed a cell-free, miniaturized enzymatic digestion system that utilizes three serial micro-mixers to simulate the digestive functions of the mouth, stomach, and small intestine.[178] They employed compounds such as starch and casein as model nutrients to assess the enzymatic digestion capabilities of the system. The results indicated that the miniaturized system significantly accelerated the digestion process compared with traditional batch digestion methods. This enzymatic digestion chip could be integrated with GLOC in the future, providing a more accurate platform for studying nutrient absorption by simulating a more realistic human digestive system.

The GLOC model, as a high-fidelity *in vitro* research platform, has become a cornerstone in studying diseases related to the gut–liver axis. Its primary value lies in its precise recapitulation of the complex physiological microenvironment and interactions between the gut and liver, including the gut microbiota, intestinal epithelial barrier, portal circulation, and hepatic metabolic functions.[179,180] By dynamically simulating the absorption of exogenous substances (*e.g.*, drugs, toxins) in the intestine and their subsequent transfer along the gut–liver axis, this model offers novel perspectives on the mechanisms underlying pathologies such as intestinal barrier dysfunction, hepatic steatosis, and chronic inflammation.[79,181] Jeon *et al.* advanced this field by developing an integrated microphysiological system encompassing the gut, liver, and immune components to investigate inflammatory responses along the gut–liver axis.[182] This system accurately models intestinal barrier function, hepatic metabolic activity, and immune cell-mediated inflammatory signaling, providing an innovative platform for elucidating the pathogenesis of gut–liver axis-related diseases and offering new avenues for research. In addition, the "metastasis chip" system developed by Skardal *et al.* is an innovative *in vitro* platform that enables real-time tracking of the migration process of fluorescently labeled colon cancer cells from the intestinal structure to the liver.[183] This system uses red fluorescent protein (RFP)-labeled human colon cancer cell line HCT-116, human intestinal epithelial cell line INT-407, and human liver cancer cell line HepG2, successfully simulating key features of tumor metastasis. The model precisely reproduces the tumor cell migration from the intestine to the liver, demonstrating its significant potential in advancing cancer research and drug discovery. The GLOC model demonstrates unique advantages in investigating the mechanisms of gut–liver axis diseases and holds extensive potential for exploring complex pathological processes, including cancer. This technology establishes a robust foundation for uncovering molecular disease mechanisms, developing personalized diagnostic tools, and optimizing therapeutic strategies, thereby driving advancements in precision medicine.

4.2 Vascularization in gut–liver-on-a-chip

Vascularization is a core element of OOC systems, as it provides a network for nutrient delivery, waste removal, and gas exchange, closely mimicking *in vivo* microenvironments. Integrating vascular channels into OOC systems enhances the physiological relevance of studies on nutrient absorption, drug metabolism, and molecular transport. By embedding endothelial cells within these channels, these models more accurately replicate the *in vivo* blood–barrier interface, essential for immune cell trafficking and transporting various molecules.[184] Xu *et al.* introduced a microfluidic-based gut–vascular-endothelium–liver co-culture chip to study the biotransformation of fluorotelomer alcohols (FTOHs) (Fig. 5c).[168] The study revealed that endothelial cells are involved in the metabolism of FTOHs. In contrast, intestinal and hepatic epithelial cell transformations produced the toxic metabolite perfluorocarboxylic acid (FTCA), further impacting angiogenesis. Additionally, it was observed that a ramped culture approach could accelerate epithelial cell proliferation and differentiation, forming a thicker cell layer resembling normal intestinal villi and enhancing intercellular communication. Exposure to high concentrations of FTOHs significantly affected cell morphology and function, including an inhibition of chamber formation and disruption of intestinal and hepatic cell differentiation, leading to irregular and loose cell arrangements. These findings offer an advanced alternative model for studying pollutant

exposure and its applications in biomedical and pharmaceutical research. In contrast to Xu *et al.*, Vernetti *et al.* focused on the coupling effects between multiple organs, proposing a four-organ functional coupling human MPS model.[185] This model includes the human intestine, sequentially layered self-assembled liver, vascularized or non-vascularized proximal renal tubules, and a complete blood–brain barrier/neurovascular unit. They tracked the absorption, metabolism, and excretion processes across these interconnected systems. The results indicated that the specific processing of these compounds across different organs aligned with clinical data.

The introduction of vascular networks in OOC systems facilitates the study of angiogenesis, a crucial process in liver regeneration, tumor growth, and the pathogenesis of various diseases.[186] By incorporating vascular components, researchers can examine the interactions between vascular structures and other cell types under dynamic flow conditions, such as hepatocytes and endothelial cells. Ferrari *et al.* developed a method to create perfusable, physiologically relevant vascular channels within a LOC model.[187] This approach enables the formation of circular cross-sectioned vascular channels within 3D hepatic microtissues without scaffolding materials. The researchers designed and validated two LOC models to replicate hepatic sinusoidal structures *in vitro*: a direct-contact platform and an ECM-mediated-contact platform. In the ECM-mediated-contact platform, a 100 μm-thick collagen–fibrin layer mimics the space of Disse, the region between hepatocytes and endothelial cells. Experiments demonstrated that hepatocytes in the ECM-mediated-contact platform exhibited higher albumin production rates and CYP3A4 activity than those in direct-contact models, underscoring the importance of simulating the space of Disse to enhance the functionality of LOC models. These findings pave the way for further applications of microfluidic technology and vascularized tissue models, including studies on interactions between vascularized organs in multi-organ chips. In addition, Yoshimoto *et al.* investigated the effects of cyclic stretching on vascular signaling secretion in hepatoblast-like cells derived from human pluripotent stem cells.[188] Using an OOC platform to simulate *in vivo* mechanical environments, they examined the influence of cyclic stretching on vascular signaling in KDR− and KDR+ cells. The results demonstrated that cyclic stretching significantly upregulated gene expression associated with epithelial–mesenchymal transition, including HGF and matrix metalloproteinase 9. Notably, these genes showed marked upregulation in co-cultured KDR− and KDR+ cells, an effect absent in monocultures. This study offers new insights into the mechanistic roles of mechanical forces during the hepatoblast stage.

Vascularization within OOC systems is essential for maintaining cellular viability and functionality. It provides a platform for investigating complex physiological and pathological processes related to the gut–liver axis. The integration of vascular components enhances these models' predictive power and relevance to human physiology, making them promising drug development and disease tools.

5. Application

5.1 Applications of gut-on-a-chip

With the advancement of microfluidic GOC models, the development of pathological models for various gastrointestinal diseases has become a prominent application. These models have proved capable of simulating key features of human gastrointestinal disorders, including IBD and small intestinal bacterial overgrowth resulting from intestinal obstruction.[84,189] These chip systems allow for the direct characterization of disease phenotypes while integrating diverse cell combinations. By controlling different pathogenic factors—such as mechanical forces, chemical gradients, and cell types—they enable an in-depth investigation of disease mechanisms and progression.[69,84,190,191]

R. Villenave *et al.* utilized Coxsackievirus B1 (CVB1) as a prototype enteric virus model to demonstrate that human enteric virus infections, including the replication and production of infectious viruses, can be analyzed *in vitro* using microfluidic GOC devices.[88] The device supports cultivating highly differentiated human villous intestinal epithelial cells under fluid flow and peristaltic-like motion.[70] When CVB1 is introduced into the epithelium-lined intestinal lumen of the device, the virus infects the epithelial cells, replicates within them, and induces detectable cytopathic effects (CPE). Additionally, infectious viral particles and inflammatory cytokines were detected in the effluent from the epithelial microchannels, indicating their release from the apical surface of the cells. This suggests that the GOC provides a suitable *in vitro* model for studying enteric virus infections and the pathogenesis of enteric viruses. Building on research into enteric viruses, organ-on-chip technology has also been employed to model the effects of other viral infections on the intestine, such as the intestinal response to SARS-CoV-2 infection. Guo *et al.* constructed a biomimetic human intestinal chip to model the intestinal response to SARS-CoV-2 infection.[97] The findings demonstrated that viral infection significantly impacted the morphology and function of intestinal epithelial cells, resulting in compromised barrier integrity, disorganized distribution of mucus-secreting cells, and reduced expression of tight junction proteins. Additionally, endothelial cells exhibited morphological damage, though with lower infection levels. Transcriptomic analysis further revealed aberrant RNA and protein metabolism in both epithelial and endothelial cells, accompanied by marked activation of immune responses post-infection. This study provides valuable data on the mechanistic role of COVID-19 infection in the intestine, offering new insights into the pathophysiology and potential therapeutic targets of SARS-CoV-2 in the gastrointestinal tract.

Beaurivage *et al.* developed a high-throughput 3D intestinal chip model based on the OrganoPlate platform, successfully replicating key pathological features of IBD (Fig. 6a).[192] By inducing Caco-2 cells to form a tubular structure of the intestinal epithelium and introducing bidirectional flow in microfluidic channels, this model effectively simulated intestinal peristalsis and vascular flow, providing a more physiologically rele-

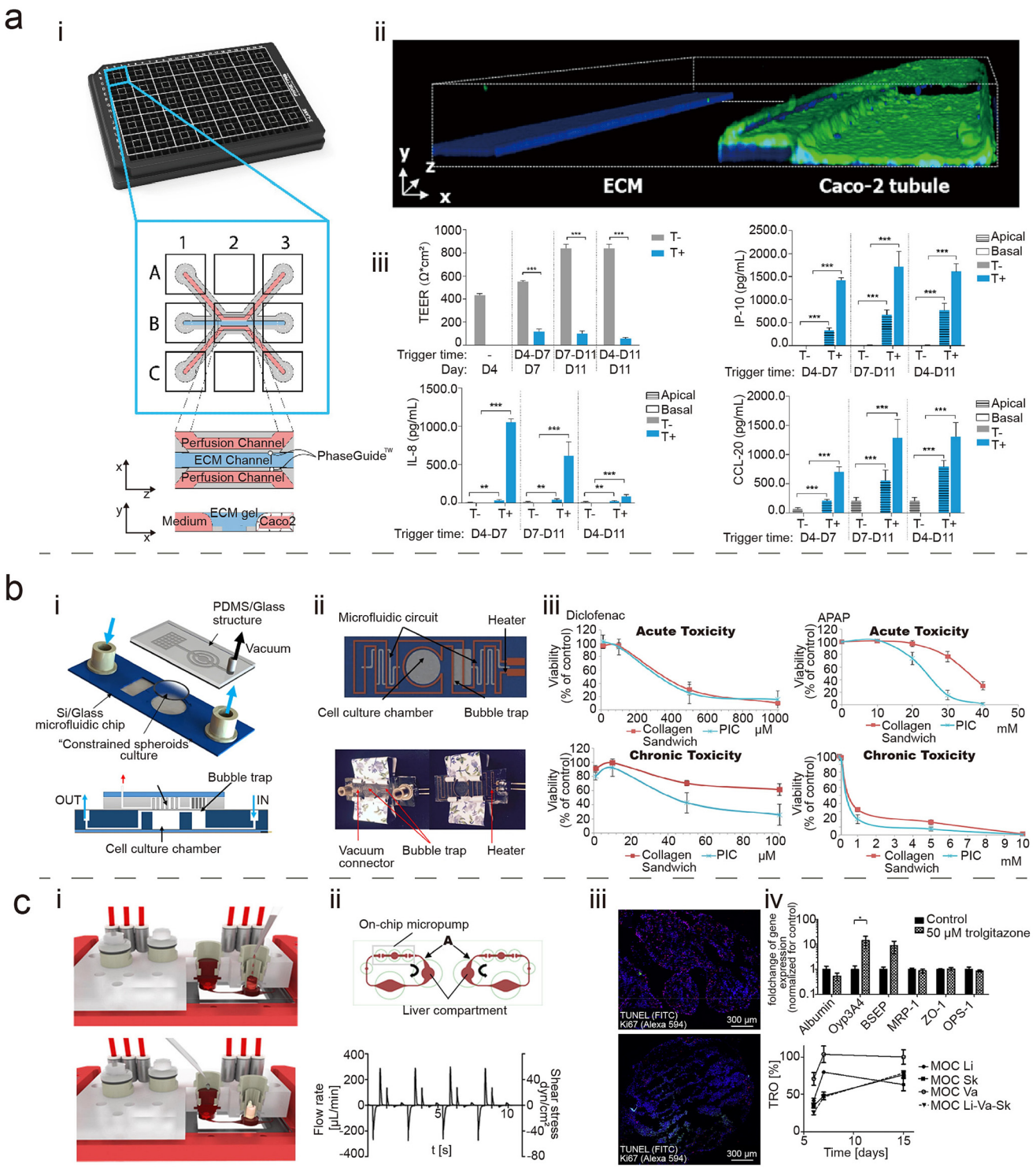

Fig. 6 Applications of the GLOC. (a) The Caco-2 tube model for IBD. (i) This model is a 3-channel OrganoPlate system consisting of 40 microfluidic chips arranged at the bottom of a standard 384-well plate format. (ii) Day 4: 3D reconstruction of Caco-2 cell tubular structure: actin (green) and DNA (blue) staining. (iii) The TEER value of Caco-2 cell tubes and the secretion dynamics of IP-10, IL-8 and CCL-20. (Reprinted with permission from ref. 192. Copyright 2019, MDPI). (b) The LOC for chronic hepatotoxicity testing. (i and ii) The chip comprises a glass/silicon structure, including 3D microfluidic circuits, cell culture chambers, bubble capture chambers, and heaters. (iii) Comparison of acute and chronic dose responses of collagen sandwich and PIC to diclofenac and APAP. (Reprinted with permission from ref. 194. Copyright 2017, Springer Nature). (c) Drug testing platform for co-culture GLOC. (i) and (ii) are cross-sectional views of the assembled MOC, illustrating the hepatic–intestinal co-culture (i) and hepatic-skin co-culture (ii) in the right circuit of each MOC. (iii) TUNEL/Ki67 staining of co-cultured liver equivalents: control and 50 μM troglitazone treatment. (iv) qRT-PCR analysis of coculture liver tissue and troglitazone concentration dynamics. (Reprinted with permission from ref. 195. Copyright 2015, Elsevier).

vant environment compared with unidirectional flow in conventional gut and liver models. The bidirectional flow better simulated food digestion and intestinal content movement and played a critical role in maintaining intestinal epithelial health and functionality. The circulating medium facilitated the exchange of cells with oxygen and nutrients, creating a microenvironment that mimics the dynamic fluid and gas exchanges in the human intestine. Under inflammatory stimulation, the TEER of Caco-2 cells significantly decreased, and there was a notable increase in the secretion of inflammatory factors, such as IP-10, IL-8, and CCL-20, particularly from the basal side, mirroring *in vivo* inflammatory processes. This model demonstrated high efficacy in simulating IBD pathophysiology and barrier dysfunction, offering a robust platform for drug screening and aiding research into ADME processes. It represents a powerful tool for studying intestinal diseases and drug development. In addition to IBD models, environmental enteric dysfunction (EED) represents another key application area for OOC technology. EED is an inflammatory intestinal disorder closely associated with malnutrition, often resulting in stunted growth in children and limited response to conventional treatments. Developing *in vitro* models that accurately simulate the pathological features of EED is therefore critical for understanding disease mechanisms and devising therapeutic strategies. Bein *et al.* developed an intestinal chip model for studying EED,[193] a chronic inflammatory condition linked to malnutrition and stunted growth in children. The study demonstrated that depleting key nutrients, such as niacinamide and tryptophan, in the chip medium could recapitulate the characteristic genetic and phenotypic features of EED. The model exhibited significant villus atrophy, impaired barrier function, and altered nutrient absorption, mirroring clinical symptoms in EED patients. Moreover, elevated secretion of inflammatory cytokines provided further insights into the disease's pathogenesis and potential therapeutic targets. This platform is a valuable tool for studying EED pathogenesis and drug development, supporting efforts to devise new treatments for this condition.

Another intriguing application of GOC pathological models is the study of the effects of radiation therapy. Jalili-Firoozinezhad *et al.* developed a GOC model to simulate the radiation damage response of the human intestine to γ-radiation, including cell death, villous blunting, and impaired barrier function. This model is used to evaluate the efficacy of radioprotective agents *in vitro*.[49] The device consists of a layer of PDMS membrane, with human intestinal epithelial cells cultured on one side and vascular endothelial cells on the other. When the GOC was exposed to γ-radiation, researchers observed an increased production of reactive oxygen species (ROS), cytotoxicity, apoptosis, DNA fragmentation, villous blunting, disruption of tight junctions, and impaired intestinal barrier integrity. Using this device as a screening platform, researchers identified that dimethyloxalylglycine (DMOG) significantly inhibited these damage responses, indicating its potential as an effective radioprotective agent. Moreover, this model further demonstrated the potential of GOC technology in discovering novel medical countermeasures (MCM).[196]

Lastly, developing *in vitro* gut microbiome models has gained significant attention recently. Research highlights the gut microbiome's close associations with diabetes treatment, cancer therapy, and other areas.[197,198] The gut microbiota is a complex ecosystem that maintains a symbiotic relationship with humans and is crucial for overall health.[199] Therefore, developing *in vitro* gut microbiome models is of significant importance. Pedicord *et al*. discovered that the symbiotic bacterium Faecalibacterium prausnitzii enhances intestinal barrier function and improves host tolerance to Salmonella typhimurium and Clostridium difficile through its secreted SagA protease.[200] SagA upregulates the expression of antimicrobial peptides and mucins, thereby limiting pathogen invasion. This mechanism can be transferred to other probiotics, highlighting its potential for preventing intestinal infections. In addition to investigating the role of commensal microbiota in intestinal function, there is growing interest in the potential of probiotics to restore gastrointestinal barrier integrity and modulate intestinal inflammation. Min *et al.* developed a leaky gut chip model to evaluate the therapeutic efficacy of live probiotics in treating compromised epithelial barriers and mucosal inflammation.[89] The study demonstrated that treatment with LGG or a multi-strain mixture (VSL#3) significantly improved barrier function, enhanced tight junction protein expression, increased mucus secretion, and reduced inflammatory marker expression in the chip model. These findings suggest the therapeutic potential of probiotics in restoring gastrointestinal barrier function and alleviating inflammatory responses, providing a novel approach and a robust validation platform for managing gastrointestinal diseases.

The GOC system offers a novel platform for *in vitro* drug screening. The GOC represents a highly biomimetic *in vitro* platform capable of accurately replicating the human intestine's complex structural and functional characteristics, including epithelial barrier function, microenvironmental conditions, and drug metabolism pathways. Compared with conventional *in vitro* models, GOC systems dynamically recreate the gut's fluidic environment and incorporate multiple cell types to emulate physiological conditions better. In early studies, Guo *et al.* developed a biomimetic human GOC to investigate drug metabolism mechanisms within the intestinal microenvironment.[201] Constructing a 3D microenvironment successfully promoted intestinal cell differentiation, significantly enhancing physiological functions. Building on this foundation, the research team introduced a universal pump-free, high-throughput 3D OOC platform for evaluating drug absorption in the intestine.[202] Their findings demonstrated that this platform could precisely simulate intestinal metabolic properties, providing a highly biologically active, cost-effective, and versatile *in vitro* tool for drug metabolism and absorption studies.

GOC technology demonstrates tremendous potential in the field of personalized medicine. Utilizing its high-fidelity

in vitro models, researchers can precisely evaluate the absorption efficiency and therapeutic efficacy of individualized drugs, with notable advantages in treating inflammatory bowel diseases, intestinal cancers, and disorders associated with microbial dysbiosis.[61] By integrating patient-specific genomic information, this technology can further predict drug efficacy and toxicity, significantly enhancing the precision of therapeutic strategies while reducing the incidence of adverse effects.[203] Moreover, GOC provides an efficient platform for mechanistic studies of complex diseases, driving advancements in precision medicine and laying a scientific foundation for patient-centered healthcare. Continued optimization and broader application of this technology are expected to expand the possibilities for designing personalized treatment regimens, propelling medicine toward greater precision and efficiency. The specific applications of intestinal organ chips discussed in Section 5.1 have been summarized in Table 3.

5.2 Applications of liver-on-a-chip

The liver is the primary metabolic organ in the human body and plays a crucial role in drug metabolism, rendering it particularly susceptible to drug-induced toxicity. Drug-induced liver injury is a leading cause of failure in late-stage drug development. Microfluidic-based *in vitro* LOC systems offer a more accurate simulation of the physiological and pathological characteristics of the human liver, providing a reliable experimental platform for drug screening and research.

Liu *et al.* established an LOC model using primary mouse hepatocytes and blood cells to simulate acute drug-induced liver toxicity and the therapeutic response to metabolic-associated steatotic liver disease (MASLD).[204] In this model, the research team first optimized protocols for isolating hepatocytes, hepatic stellate cells, Kupffer cells, and hepatic sinusoidal endothelial cells from mouse livers, and co-cultured these cells with circulating immune cells on a bilayer microchip. By introducing APAP and FFA, they successfully simulated the pathological features of acute drug-induced liver injury and MASLD. Experimental results demonstrated that the LOC model effectively recapitulated key features of MASLD, including cell death, lipid accumulation, and inflammatory responses. Moreover, the model evaluated the therapeutic effects of two drug candidates, lanifibranor and resmethrin, significantly reducing lipid accumulation and inflammation in hepatocytes. This study highlights the significant application potential of the LOC model in drug screening and liver disease research. Building upon Liu *et al.*'s success in modeling acute drug-induced liver injury and fatty liver, Yu *et al.* further expanded the application of LOC technology by designing a perfusion-incubator-liver-chip (PIC) optimized for evaluating long-term drug toxicity responses (Fig. 6b).[194] The study demonstrated that hepatocytes cultured in the PIC system showed greater sensitivity to chronic toxicity from diclofenac sodium and acetaminophen compared with a conventional collagen sandwich culture. Specifically, in the diclofenac sodium assay, the PIC system's half-maximal inhibitory con-

Table 3 Application of GOC

Cell type	Platform	Tissue structure	Application	Ref.
Caco-2	2-Channel PDMS microporous	Spontaneous formation of intestinal villi	Creating a model of human intestinal disease	84
Caco-2, HIMEC	2-Channel PDMS microporous	The cells form the villous intestinal epithelium	As a discovery tool for developing microbiome-related therapeutics, probiotics and nutraceuticals	69
Caco-2	2-Channel PDMS microporous	The villous structure is about 50–100 μm high, and the polarized epithelial cells contain microvilli of villus proteins	Providing an *in vitro* model for enterovirus infection, study of enterovirus pathogenesis	88
Caco-2; HT-29; HUVEC	2-Channel PDMS microporous	Forming intestinal epithelial–endothelial barrier. Epithelial cells form villus-like structures	Providing a platform to accelerate COVID-19 research and development of new treatments	97
Caco-2	3-Channel ECM gel	Forming a complete and polarized leak-tight tubule	Expanding the method for disease modeling, target validation, and drug discovery	192
Biopsy samples from EED patients	2-Channel PDMS microporous	Forming a 3D villus structure. Producing a mucus layer	Helps analyze the molecular, genetic, and nutritional basis of EED and test candidate therapies for it	193
Caco-2; HUVECs	2-Channel PDMS microporous	Forming a 3D villus structure and a confluent cell monolayer	As an *in vitro* platform to study radiation-induced cell death and associated gastrointestinal acute syndromes	49
Caco-2	2-Channel PDMS microporous	Recreating 3D layers of human intestinal Caco-2 epithelial cells	Providing a translational strategy to dissect the therapeutic mechanisms of living biotherapeutic products	89
Caco-2	1-Channel PDMS microporous	Forming a confluent epithelial monolayer with tight junctions	Providing an *in vitro* platform for intestinal metabolism research and preclinical drug development	201
Caco-2	3D-High throughput	Forming of 3D villus-like structure	The potential of tools to advance drug development and enable personalized medicine	202

Human intestinal microvascular endothelial cells (HIMEC).

centration (IC_{50}) was 50.86 μM, significantly lower than the 121.53 μM observed in collagen sandwich cultures. In the acetaminophen test, 1 mM of acetaminophen reduced cell viability to 21% in the PIC system, compared with 32% in collagen sandwich culture, with IC_{50} values of 2.391 mM and 3.059 mM, respectively. These findings indicate that the PIC system offers significant advantages for long-term drug toxicity testing, providing a more sensitive and stable model for chronic toxicity assessment. To evaluate the chronic effects of drugs on the liver, *in vitro* LOC models must support long-term culture while maintaining liver-specific functionality, stability, and viability over extended periods. Messner *et al.* developed a 3D liver model consisting of primary human hepatocytes and non-parenchymal cells, which they employed for long-term testing and to assess inflammation-mediated toxicity.[205] This model enables liver microtissues to maintain stable activity and function for up to five weeks, allowing for the assessment of chronic drug effects. Docci *et al.* conducted in-depth research in this field and developed a liver chip device called PhysioMimix.[206] This system combines mathematical modeling and simulation techniques to provide an innovative platform for quantitatively studying drug metabolism. Experimental results confirmed that the device offers significant advantages in simulating liver metabolic characteristics, particularly in evaluating the activity of various drug-metabolizing enzymes, such as cytochrome P450, UDP-glucuronosyltransferase, and aldehyde oxidase, with high precision. The study also emphasized the crucial role of mathematical modeling in enhancing parameter calculation accuracy, assessing metabolic and transport processes, and managing heterogeneous drug concentration distributions. Notably, in complex cellular systems, drug evaporation and sampling effects are often difficult to quantify; however, PhysioMimix successfully addresses this challenge through its precise model analysis capabilities.

As the understanding of liver diseases and toxicity mechanisms deepens, increasing efforts are being made to simulate cellular-level responses in the liver using advanced technologies. Compared with traditional liver models, the LOC system developed by Huh *et al.*, based on 3D bioprinting technology, offers greater precision, especially in simulating acute toxic responses and drug screening, demonstrating exceptional potential.[207] They developed a 3D bioprinted LOC system using human liver spheroids with GelMA-based bioink. This system showed excellent cell viability, sustained ATP production, and albumin secretion over 14 days. The study demonstrated that the 3D-printed liver chip system could effectively identify hepatotoxicity induced by APAP and successfully model acute liver failure caused by APAP overdose. These findings highlight the potential applications of this *in vitro* model in high-throughput drug screening, precise biological process studies, and monitoring tissue responses to drugs. To further enhance the capability of *in vitro* models in mimicking the complex hepatic microenvironment, Zheng *et al.* designed and fabricated an integrated 3D dynamic multicellular LOC (3D-DMLOC) that successfully replicates the *in vivo* liver microenvironment, including hepatic sinusoids, the perisinusoidal space, and continuous fluid perfusion, to improve the reliability of hepatotoxicity screening.[208] The research team validated the device's functionality by co-culturing HepaRG and HUVEC cells within this chip. Experimental results demonstrated that, compared with traditional static culture, co-cultured cells in the 3D-DMLOC expressed elevated levels of hepatic polarity proteins (ZO-1 and MRP2) and functional liver markers (ALB, UREA, and CYP450 enzymes). Moreover, the model exhibited greater sensitivity to toxins, indicated by a significant increase in LDH release from hepatocyte spheroids, underscoring the 3D-DMLOC system's enhanced accuracy and reliability in screening potential hepatotoxic compounds. Recent studies have increasingly focused on optimizing long-term culture environments to enhance model stability and functionality. For example, Rajan *et al.* developed a novel microfluidic liver tissue chip (LTC) with continuous medium recirculation, using PHH and optimizing it for extended liver culture.[209] This chip demonstrated low nonspecific binding to various ionic states and lipophilic drugs while maintaining cytochrome P450 metabolic activity for at least 15 days, preserving hepatocyte functionality and polarity. In drug clearance studies, the LTC enabled continuous drug metabolism assessments for at least 12 days and successfully estimated clearance rates with high *in vivo–in vitro* correlation (IVIVC) for multiple compounds. By leveraging advances in bioengineering, this study developed a highly reproducible, low-variability platform that addresses long-standing challenges in pharmacokinetics research, particularly in accurately predicting drug clearance, demonstrating significant potential in this domain.

Liver diseases are a leading cause of mortality worldwide, and environmental factors increasingly aggravate this problem. Deepening our understanding of liver physiology is essential for uncovering the mechanisms underlying liver diseases, improving treatment strategies, and enhancing predictive capabilities for disease progression and drug responses. However, a key challenge remains in accurately recreating the complexity of liver structure and function *in vitro*. Therefore, there is an urgent need for the development of advanced preclinical models to study the mechanisms of liver diseases.[210]

One of the most common liver diseases is NAFLD, which is among the most prevalent chronic liver conditions globally, especially in developed countries.[211] The progression of NAFLD can range from simple steatosis to non-alcoholic steatohepatitis (NASH), which can further advance to cirrhosis and ultimately lead to HCC. HCC is one of the top three causes of cancer-related deaths worldwide, making early diagnosis of NAFLD as a potential risk factor crucial.[212] However, many *in vitro* studies on NAFLD are limited by the constraints of 2D culture systems. To address this issue, Gori *et al.* developed a 3D microfluidic model of NAFLD.[213] They introduced palmitic acid and oleic acid as high-level FFA into the LOC to assess intracellular lipid accumulation, cell viability/toxicity, and oxidative stress induced by FFA overload. Compared with 2D static cultures, this chip facilitates a gradual reduction in intracellular lipid accumulation, improves hepatocyte survival, and

Table 4 Application of LOC

Cell type	Platform characteristics	Tissue structure	Application	Ref.
Mouse primary hepatocytes; HSC; KC; LSEC	Dual-chamber structure	2D structural monolayers	Recapitulating drug-induced liver injury and MASLD-related features	204
Rat hepatocytes	Perfusable	3D hepatocyte spheroids	Long-term cell culture, repeated dosing tests	194
PHH; KC; EC	96-Well format	3D liver microtissues	Conventional compound testing, inflammation-mediated toxicity	205
Hepatocytes	Media flow	—	Studying the distribution characteristics of drug candidates in the liver *in vitro*	206
HepG2	3D bioprinted tissue	3D hepatic tissue spheroids	High cell viability, simulating acute liver failure	207
HepaRG; HUVEC	9 × 9 pinhole array	3D hepatocyte spheroids	*In vitro* hepatotoxicity screening	208
PHH	Continuous media recirculation	Morphology of characteristic cobblestone	Predicting pharmacokinetics	209
HepG2; C3A cells	Microarchitecture resembling human liver sinusoids	HepG2 cells form small aggregates	Establishing an *in vitro* model of human NAFLD	213
Rat primary hepatocytes; HSCs	A concave–convex structure	3D co-culture spheroids exhibit fibrous structures	Drug screening, studying ALI-related mechanisms *in vitro*	214
HepDE19; PHH; HepG2; KC	Nutrients and oxygenated culture medium can be continuously recycled	Forming of hepatic cell microtissues	Studying hepatitis B virus, other hepatotropic pathogens, liver biology, and drug development	215

minimizes oxidative stress under dynamic microfluidic conditions, thereby more closely mimicking the chronic state of steatosis observed *in vivo*. This provides a more reliable model for studying the pathogenesis of NAFLD. In addition to NAFLD, models for other liver diseases have also been progressively developed. For example, models have been established for alcoholic liver disease (ALD), hepatitis B virus (HBV) infection, and HCC.[214,215] These models provide valuable tools for studying liver disease progression, advancing drug discovery, and conducting toxicity testing. The simulation systems on liver chips offer significant promise for research into liver diseases and potential treatments. The specific applications of LOC discussed in Section 5.2 have been summarized in Table 4.

5.3 Applications of gut–liver-on-a-chip

The homeostatic relationship between the gut, microbiome, and liver plays a crucial regulatory role in drug metabolism. It is well established that the gut microbiota significantly influences human health and disease by enhancing food metabolism and acting as the first line of defense against pathogens. In addition, the gut microbiome is essential in metabolizing exogenous pharmaceutical compounds. However, simulating the highly dynamic intestinal environment and understanding how the gut microbiota modulates drug bioavailability and contributes to liver toxicity remain significant challenges.[216]

Many diseases involve complex mechanisms across multiple organs, making establishing accurate models of these conditions challenging. OOC technology offers the opportunity to simulate the physiological microenvironments of *in vivo* tissues. Connecting these "organ modules", it is possible to recreate interactions between organs.[217] Yang *et al.* developed an integrated gut–liver-on-a-chip (iGLOC) as an *in vitro* human model for simulating NAFLD.[218] This platform utilizes microfluidic technology to co-culture Caco-2 and HepG2 cells, recreating the gut–liver axis and enabling the modeling of NAFLD onset and progression through FFA treatment. Findings indicate that, compared with monoculture systems, co-cultured cells exposed to FFA exhibit reduced apoptosis and a significant increase in lipid droplet accumulation. Furthermore, genes associated with copper ion response and endoplasmic reticulum stress were upregulated. These results suggest that the iGLOC platform may be an alternative to animal models for investigating NAFLD pathogenesis, offering novel insights for drug development, therapeutic strategies, and diagnostic tool exploration. This technology offers a novel approach for studying the interactions of multi-organ systems in disease processes.

Maschmeyer *et al.* employed advanced microphysiological system technology to design and implement a miniature *in vitro* gut–liver co-culture model that simulates the gut–liver interactions observed in living organisms (Fig. 6c).[195] This platform enables the long-term co-culture of human liver organoids with intestinal or skin barrier models, maintaining stability for up to 14 days. In their study, liver organoids exhibited expected toxic responses to troglitazone exposure, including increased apoptosis and elevated CYP3A4 mRNA expression, indicating drug-induced biotransformation activity. Furthermore, experimental data showed a rapid decrease in troglitazone concentration in the culture medium during the initial treatment phase, suggesting substantial tissue drug absorption. These results validate the multiorgan-on-a-chip (MOC) platform's effectiveness in simulating drug metabolism and toxicity, presenting a promising alternative to animal testing for drug and substance safety evaluation.

The GLOC is an innovative microfluidic technology that can simulate drug metabolism processes in the liver. Jie *et al.* introduced an innovative GLOC designed as a drug screening

Table 5 Progress towards replication of the gut–liver axis *in vitro*

Application	Cell type	Description	Finding	Ref.
Four-organ-chip for *in vitro* microfluidic ADME profiling	EpiIntestinal™, HepaRG, HHSC, HJP, human proximal tubule cell	Microfluidic four-organ-chip	The model simulates physiological absorption, metabolism in liver tissue, and ultimately excretion through the kidneys	165
GLOC for disease models	Caco-2, HepG2	Microfluidic GLOC	Gut absorption of fatty acids and hepatic lipid accumulation are enhanced under dynamic conditions	167
Intestinal and liver slices for first-pass metabolism	Rat intestinal slices, rat liver slices	Microfluidic-based *in vitro* system	The substrates tested showed results in this system that were consistent with the validated data	169
GLOC for drug screening	Primary human intestinal cells, human intestinal myofibroblasts, HepG2 C3A	Modular gastrointestinal tract–liver system	Demonstration of 28-day gastrointestinal tract–liver systemic co-culture using gravity-induced oscillatory bidirectional fluid flow	170
Gut–liver fluidic platform for PK	PHH, KC, Caco2	Integrated gut–liver multiple MPS	*In vitro* system can detect diclofenac primary metabolites in humans	172
GLOC for mimicking the organ–organ interactions	Caco-2, HepG2 C3A	Microfluidic GLOC	The function of intestinal epithelial cells was maintained. The activity of CYP1A enzyme in the liver was increased	174
GLOC for ADME	Caco2, HT29, hepatocytes	Gut–liver MPS	Capturing the intestinal and hepatic metabolism of mycophenolate mofetil	175
Gut–liver axis platform for drug metabolism	Caco-2, HepaRG, HUVEC, THP-1	Microfluidic gut–liver axis platform	Models the bidirectional connection between the gut and liver	26
Gut–liver axis chip for disease models	Caco-2, HepG2, RAW264.7	Three-tissue MPS	Reproducing an inflammatory response involving the gut, liver, and immune cells	182
GLOC for disease models	HCT-116, INT-407, HepG2	Microfluidic GLOC	HCT-116 cells can spontaneously shed into the blood circulation	183
3D intestine–vessel–liver chip for toxicity testing	HepG2, HCT-116, HUVEC	Microfluidic 3D intestine–vessel–liver chip	The barrier function of HCT116 cells was impaired, HUVEC growth was restricted, and HepG2 cells may suffer from oxidative stress after FTOH exposure	168
MOC for assessing repeated-dose safety	HepaRG, HHSC, small intestine epithelial cells, HJP	Microfluidic MOC	Human 3D liver equivalents were co-cultured with the intestinal barrier model for 14 days	195
GLOC for drug metabolism	HepG2, Caco-2	Microfluidic GLOC	High concentrations of combined drugs can inhibit cell growth and metabolic capacity	219
GLOC for first-pass metabolism	Caco-2, PHH	Microfluidic GLOC	Coadministration of metabolic inhibitors may inhibit liver metabolism	220
GLOC for toxicokinetic	Caco-2, HT29-MTX-E12, HepG2, HUVEC-T1, THP-1, HHSC	Gut–liver MPS	APAP treatment increased the hepatotoxicity markers AST and ALT levels, decreased ALB secretion, inhibited cell proliferation, and enhanced ROS	221

Human primary hepatic stellate cells (HHSC), human juvenile prepuce (HJP).

platform to simulate the absorption and metabolism of orally administered drugs in the gut and liver.[219] The platform features a dual-layer design combined with hollow fiber technology, successfully reconstructing the physiological functions of the gut and liver at a microscale. The upper layer of the hollow fibers is seeded with Caco-2 cells to simulate the intestinal epithelium. At the same time, the lower chamber is cultured with HepG2 cells to represent liver tissue, forming a dynamic co-culture system. The study results indicate that cell viability and metabolic activity were not significantly affected within a specific concentration range (<100 μg mL^{-1}), suggesting that HepG2 cells retained their drug metabolism capabilities at these concentrations. When drug concentrations exceeded 250 μg mL^{-1}, apoptosis was observed, validating the model's effectiveness in assessing drug toxicity. The GLOC platform enables dynamic monitoring of drug absorption and metabolism. It facilitates long-term observation, providing a powerful tool for an in-depth understanding of drug mechanisms and drug–drug interactions. Amid the ongoing advancements in gut–liver chip technology, further optimization of materials and design holds significant potential for enhancing the accuracy of drug metabolism simulations. In this context, Wang *et al.* developed a GLOC system based on perfluoropolyether, which effectively addresses drug adsorption issues and enables a more precise assessment of drug metabolism and bioavailability.[220] Their study demonstrated that, compared with polydimethylsiloxane-based chips, the perfluoropolyether-based chip showed over a 20-fold increase in the presence of intact midazolam in the liver chamber effluent, confirming the saturation of hepatic metabolism at higher concentrations. Additionally, co-administration with ketoconazole significantly inhibited metabolism, highlighting the chip's potential for evaluating drug–drug interactions and performing individualized assessments of intestinal and hepatic drug availability. To further advance the application of gut–liver chips in drug metabolism and toxicity evaluations, researchers continue to optimize system design and incorporate additional cell types to more accurately model complex physiological pro-

cesses. Yu *et al.* developed an MPS, termed the GLOC, designed to simulate drug absorption and metabolism as well as to predict pharmacokinetics and toxicological responses following acetaminophen overdose.[221] They constructed an intestinal equivalent using Caco-2 and HT29-MTX-E12 cell lines, while the liver equivalent was established using HepG2, HUVEC-T1, PMA-induced THP-1 cells, and human hepatic stellate cells. The study demonstrated that this system could detect acute liver injury processes, track changes in liver injury biomarkers, and assess drug-induced toxicity, thus underscoring the utility of OOC technology in drug toxicity evaluation. Compared with traditional 2D or 3D cell cultures, this chip technology more accurately reflects the *in vivo* environment, reducing the need for animal testing, improving screening efficiency and predictive accuracy, and laying a solid foundation for subsequent preclinical studies and developing personalized medical strategies. We have summarized the research progress on replicating the gut–liver axis *in vitro* in Table 5.

6. Challenges and future directions

Despite significant advancements in the *in vitro* simulation of the GLOC platform, the field still faces several challenges. Continued investment in design and development is essential to overcome these hurdles and improve the practicality and effectiveness of these devices in both industrial and clinical settings.

Currently, PDMS is one of the most widely used materials in OOC applications due to its biological inertness, low cost, and excellent transparency.[222] However, this polymer has some notable drawbacks, such as its tendency to adsorb hydrophobic small molecules, resulting in the absorption of lipophilic compounds onto the device walls.[223,224] In addition, drugs or fluorescent molecules co-incubated with cells may diffuse into the PDMS device, thereby reducing the reproducibility of solute concentrations in the solution.[225] Therefore, utilizing alternative polymers such as polyurethane or styrene block copolymers or implementing surface modifications based on ECM materials can effectively address these issues.[226,227]

In terms of cell selection, many studies have opted for immortalized cell lines; however, their biological characteristics differ significantly from those of human cells *in vivo.*[228] In contrast, using human pluripotent stem cells (hPSCs) in GOC models provides a more accurate *in vitro* reconstruction of physiological responses, enhancing the models' physiological relevance and predictive capacity.[229] However, while hPSCs offer a closer approximation to *in vivo* environments, they may result in shorter device lifespans, which limits their application in long-term experiments.[230] Additionally, current GOC models often simulate only a limited layer of the intestinal wall and fail to replicate the *in vivo* gut microphysiological environment fully. For example, these models typically lack the involvement of smooth muscle cells and enteric neurons, which play crucial roles in gut function. Smooth muscle cells regulate the production of glial cell-derived neurotrophic factors through the expression of Toll-like receptors 1–9, affecting neuronal integrity and consequently controlling intestinal secretion, blood flow, and motility.[231,232] Future advancements in GOC applications could utilize self-organizing or directed differentiation techniques to convert induced pluripotent stem cells (iPSCs) into functional smooth muscle cells, thereby reconstructing a more complete intestinal structure.[233] This would increase the functional complexity of the gut model and allow for a more precise simulation of both the physiological and pathological states of the gut. Therefore, to enhance the physiological relevance of models and better reflect the complexities of intestinal function, future research should focus on incorporating additional cell types, particularly smooth muscle cells and enteric neurons, to more comprehensively simulate the multi-layered physiological processes of the gut and provide more realistic platforms for disease research.

In addition to improving cell sources and types, integrating microbiota presents numerous challenges and issues. In the human body, gut microbiota coexist and form a complex ecosystem, necessitating the inclusion of a broader variety of bacteria for co-culturing in GOC models. Moreover, the density and distribution of gut microbiota vary across different gut locations (*e.g.*, inflammatory sites) and change over time. However, existing GOC models lack *in situ* measurements of microbiota and host responses, leading to uncertainties in the *in vitro* simulation of intestinal diseases. To address this issue, sensors, and advanced imaging technologies to monitor tissues have been employed to gather more data, thereby enhancing the understanding of cellular behavior within the device.[234,235] Embedded electrodes for measuring TEER are widely used to quantify epithelial barrier integrity. However, additional sensors are still needed to monitor and analyze other substances in *in vitro* GOC systems.[236]

The integration of GOC and LOC models also faces several challenges. For example, the differing growth rates of gut and liver cells must be considered when performing biological scaling to ensure appropriate scaling ratios. Additionally, different channel structures require the control of distinct flow rates to accommodate the specific growth environments of the respective cells.[237] Moreover, each tissue type requires an adequate supply of specific nutrients and growth factors, making providing a universal cell culture medium another critical challenge.[163]

Most research on OOC systems remains concentrated in academic laboratories, and significant discrepancies in equipment design and experimental methodologies between laboratories have led to a lack of consistency in results and data. Additionally, the absence of standardized, universal designs and operational protocols for OOC models, combined with high manufacturing and experimental implementation costs, further limits the broader adoption of OOC systems.[238] In this context, the IQ Consortium has provided critical guidance for the development of MPS technologies, particularly highlighting their immense potential in pharmaceutical safety and ADME studies.[239] MPS technology complements existing pre-

clinical drug safety assessments. It offers unique advantages in drug safety testing for key organs such as the heart, liver, and kidneys while reducing reliance on animal models. The IQ Consortium has established a framework to guide the translation of MPS technologies from academic research to commercial applications, a framework that is equally applicable to advancing the industrialization of OOC technologies. By promoting standardized designs, reducing costs, and fostering cross-disciplinary collaboration and communication, OOC technology holds the potential for widespread use in the pharmaceutical industry, providing more efficient and operable *in vitro* drug development and safety evaluation models.

Modern OOC systems offer tremendous promise in elucidating the mechanisms behind many incurable diseases.[240] High-throughput capabilities are a crucial future direction for the development of GLOC systems. Integrating technologies such as genome editing, 3D printing, and organoid biobanks can potentially enhance automation and parallel processing capabilities. Machine learning is essential for analyzing the extensive data generated by GLOC systems, enhancing the efficiency and accessibility of data analysis.[241,242] Future GLOC systems are anticipated to decrease the number of drug candidates, expedite the preclinical screening process, and facilitate the development of personalized treatment plans.[243,244] The recent Food and Drug Administration (FDA) Modernization Act 2.0 has stimulated industrial investment in advanced *in vitro* 3D models, including organoids, spheroids, OOC systems, 3D bioprinting, and *in silico* approaches. This shift indicates that *in vitro* human models are set to become a mainstream trend in future development.[245]

Data availability

Data availability is not applicable to this article as no new data were created or analyzed in this study.

Conflicts of interest

The authors declare no competing financial interest.

Acknowledgements

The research is supported by the National Natural Science Foundation of China (No. 62371267, 62121003); Key R & D Program of Shandong Province (Major innovation project) (2022CXGC020501); Science, Education and Industry Integration Innovation Pilot Project from Qilu University of Technology (Shandong Academy of Sciences) (No. 2022JBZ02-01); Research Leader Studio in Colleges and Universities of Jinan (No. 2021GXRC083); Innovation Team of Organ-on-a-Chip Manufacturing Key Technologies (No. 202333015, Funded by Jinan Science and Technology Bureau); Young Innovative Talents Introduction & Cultivation Program for Colleges and Universities of Shandong Province (Granted by the Department of Education of Shandong Province, Sub-Title 1: Innovative Research Team of High-Performance Integrated Device, Sub-Title 2: Innovative Research Team of Advanced Energy Equipment); Shandong Provincial Natural Science Foundation (ZR2023QH405); Qilu University of Technology (Shandong Academy of Sciences) Youth Outstanding Talent Program (2024QZJH03); and Talent Research Project of the Pilot Project of Science, Education and Industry Integration (2024RCKY002).

References

1 C. L. Hsu and B. Schnabl, *Nat. Rev. Microbiol.*, 2023, **21**, 719–733.
2 S. Anand and S. S. Mande, *npj Biofilms Microbiomes*, 2022, **8**, 89.
3 K. L. Mertens, A. Kalsbeek, M. R. Soeters and H. M. Eggink, *Front. Neurosci.*, 2017, **11**, 617.
4 J. Behary, N. Amorim, X.-T. Jiang, A. Raposo, L. Gong, E. McGovern, R. Ibrahim, F. Chu, C. Stephens, H. Jebeili, V. Fragomeli, Y. C. Koay, M. Jackson, J. O'Sullivan, M. Weltman, G. McCaughan, E. El-Omar and A. Zekry, *Nat. Commun.*, 2021, **12**, 187.
5 A. Nicoletti, F. R. Ponziani, M. Biolato, V. Valenza, G. Marrone, G. Sganga, A. Gasbarrini, L. Miele and A. Grieco, *World J. Gastroenterol.*, 2019, **25**, 4814–4834.
6 J. König, J. Wells, P. D. Cani, C. L. García-Ródenas, T. MacDonald, A. Mercenier, J. Whyte, F. Troost and R.-J. Brummer, *Clin. Transl. Gastroenterol.*, 2016, **7**, e196.
7 K. Y. G. Villareal, A. R. Santillanes and B. Lazalde, *GSC Adv. Res. Rev.*, 2024, **19**, 176–181.
8 H. Mostafavi Abdolmaleky and J.-R. Zhou, *Antioxidants*, 2024, **13**, 985.
9 D. M. S. Ferreira, A. L. Simão, C. M. P. Rodrigues and R. E. Castro, *FEBS J.*, 2014, **281**, 2503–2524.
10 A. Albillos, A. De Gottardi and M. Rescigno, *J. Hepatol.*, 2020, **72**, 558–577.
11 A. Ghosh, S. Ghosh, F. Pati and S. Duraiswamy, *Bioprinting*, 2023, **36**, e00316.
12 A. Loewa, J. J. Feng and S. Hedtrich, *Nat. Rev. Bioeng.*, 2023, **1**, 545–559.
13 G. Trujillo-de Santiago, M. J. Lobo-Zegers, S. L. Montes-Fonseca, Y. S. Zhang and M. M. Alvarez, *Microphysiol. Syst.*, 2018, **2**, 7.
14 A. D. Kostic, M. R. Howitt and W. S. Garrett, *Genes Dev.*, 2013, **27**, 701–718.
15 M. Martignoni, G. M. M. Groothuis and R. De Kanter, *Expert Opin. Drug Metab. Toxicol.*, 2006, **2**, 875–894.
16 C. C. Croney and R. Anthony, *J. Anim. Sci.*, 2010, **88**, E75–E81.
17 L. Wang, J. Wu, J. Chen, W. Dou, Q. Zhao, J. Han, J. Liu, W. Su, A. Li, P. Liu, Z. An, C. Xu and Y. Sun, *Talanta*, 2021, **226**, 122097.
18 D. E. Ingber, *Nat. Rev. Genet.*, 2022, **23**, 467–491.

19 C. M. Leung, P. De Haan, K. Ronaldson-Bouchard, G.-A. Kim, J. Ko, H. S. Rho, Z. Chen, P. Habibovic, N. L. Jeon, S. Takayama, M. L. Shuler, G. Vunjak-Novakovic, O. Frey, E. Verpoorte and Y.-C. Toh, *Nat. Rev. Methods Primers*, 2022, **2**, 33.
20 C. Tian, Q. Tu, W. Liu and J. Wang, *TrAC, Trends Anal. Chem.*, 2019, **117**, 146–156.
21 D. H. Kim and J. H. Cheon, *Immune Netw.*, 2017, **17**, 25.
22 M. K. Shin, S. K. Kim and H. Jung, *Lab Chip*, 2011, **11**, 3880–3887.
23 M. L. Shuler, *Lab Chip*, 2017, **17**, 2345–2346.
24 B. A. Hassell, G. Goyal, E. Lee, A. Sontheimer-Phelps, O. Levy, C. S. Chen and D. E. Ingber, *Cell Rep.*, 2017, **21**, 508–516.
25 J. E. Sosa-Hernández, A. M. Villalba-Rodríguez, K. D. Romero-Castillo, M. A. Aguilar-Aguila-Isaías, I. E. García-Reyes, A. Hernández-Antonio, I. Ahmed, A. Sharma, R. Parra-Saldívar and H. M. N. Iqbal, *Micromachines*, 2018, **9**, 536.
26 M. Lucchetti, K. O. Aina, L. Grandmougin, C. Jäger, P. Pérez Escriva, E. Letellier, A. S. Mosig and P. Wilmes, *Adv. Healthcare Mater.*, 2024, **13**, 2303943.
27 R. McCoy, S. Oldroyd, W. Yang, K. Wang, D. Hoven, D. Bulmer, M. Zilbauer and R. M. Owens, *Adv. Sci.*, 2024, **11**, 2306727.
28 K. J. Maloy and F. Powrie, *Nature*, 2011, **474**, 298–306.
29 K. Zhang, M. W. Hornef and A. Dupont, *Cell. Microbiol.*, 2015, **17**, 1561–1569.
30 A. Fedi, C. Vitale, G. Ponschin, S. Ayehunie, M. Fato and S. Scaglione, *J. Controlled Release*, 2021, **335**, 247–268.
31 W. van Schaik, *Philos. Trans. R. Soc., B*, 2015, **370**, 20140087.
32 Y. C. Shin, N. Than, S. Min, W. Shin and H. J. Kim, *Nat. Rev. Bioeng.*, 2023, **2**, 175–191.
33 T. G. Schulman, R. S. Samlal-Soedhoe and J. van der Weerd, *Forensic Sci. Rev.*, 2018, **30**, 51–75.
34 F. Abed-Meraim and A. Combescure, *Struct. Eng. Mech.*, 2011, **37**, 253–256.
35 T. M. Schmidt and J. Y. Kao, *Gastroenterology*, 2014, **147**, 956–959.
36 J. F. Gautier, S. P. Choukem and J. Girard, *Diabetes Metab.*, 2008, **34**, S65–S72.
37 M. Nizard, M. O. Diniz, H. Roussel, T. Tran, L. C. Ferreira, C. Badoual and E. Tartour, *Hum. Vaccines Immunother.*, 2014, **10**, 2175–2187.
38 X. Pan, J. Chen, J. Han, W. Zhang, W. Su, Z. Xu, X. Li, M. Song, W. Song, X. Xie and L. Wang, *ACS Appl. Mater. Interfaces*, 2024, **16**, 51139–51149.
39 X. Ding, X. Hu, Y. Chen, J. Xie, M. Ying, Y. Wang and Q. Yu, *Trends Food Sci. Technol.*, 2021, **107**, 455–465.
40 G. Lemmens, A. Van Camp, S. Kourula, T. Vanuytsel and P. Augustijns, *Pharmaceutics*, 2021, **13**, 161.
41 M. J. Haddad, W. Sztupecki, C. Delayre-Orthez, L. Rhazi, N. Barbezier, F. Depeint and P. M. Anton, *Int. J. Mol. Sci.*, 2023, **24**, 3595.
42 B. Ferreira, A. S. Barros, C. Leite-Pereira, J. Viegas, J. Das Neves, R. Nunes and B. Sarmento, *Biochim. Biophys. Acta, Mol. Basis Dis.*, 2024, **1870**, 167042.
43 J. A. Fix, in *Models for Assessing Drug Absorption and Metabolism*, ed. R. T. Borchardt, P. L. Smith and G. Wilson, Springer US, Boston, MA, 1996, vol. 1, pp. 51–66.
44 M. A. Alam, F. I. Al-Jenoobi and A. M. Al-mohizea, *J. Pharm. Pharmacol.*, 2012, **64**, 326–336.
45 A. Lechanteur, A. Almeida and B. Sarmento, *Eur. J. Pharm. Biopharm.*, 2017, **119**, 137–141.
46 M. Chi, B. Yi, S. Oh, D. J. Park, J. H. Sung and S. Park, *Biomed. Microdevices*, 2015, **17**, 1–10.
47 V. De Gregorio, B. Corrado, S. Sbrescia, S. Sibilio, F. Urciuolo, P. A. Netti and G. Imparato, *Biotechnol. Bioeng.*, 2020, **117**, 556–566.
48 A. Grassart, V. Malardé, S. Gobba, A. Sartori-Rupp, J. Kerns, K. Karalis, B. Marteyn, P. Sansonetti and N. Sauvonnet, *Cell Host Microbe*, 2019, **26**, 435–444.
49 S. Jalili-Firoozinezhad, R. Prantil-Baun, A. Jiang, R. Potla, T. Mammoto, J. C. Weaver, T. C. Ferrante, H. J. Kim, J. M. S. Cabral, O. Levy and D. E. Ingber, *Cell Death Dis.*, 2018, **9**, 1–14.
50 J. C. Clemente, L. K. Ursell, L. W. Parfrey and R. Knight, *Cell*, 2012, **148**, 1258–1270.
51 T. Agarwal, V. Onesto, L. Lamboni, A. Ansari, T. K. Maiti, P. Makvandi, M. Vosough and G. Yang, *Bio-Des. Manuf.*, 2021, **4**, 568–595.
52 Y. C. Shin, N. Than, S. J. Park and H. J. Kim, *Expert Opin. Drug Metab. Toxicol.*, 2024, **20**, 593–606.
53 M. A. Signore, C. De Pascali, L. Giampetruzzi, P. A. Siciliano and L. Francioso, *Sens. Bio-Sens. Res.*, 2021, **33**, 100443.
54 G. M. Whitesides, *Nature*, 2006, **442**, 368–373.
55 A. Shamloo, S. Abdorahimzadeh and R. Nasiri, *AIChE J.*, 2019, **65**, e16741.
56 D. Huh, H. J. Kim, J. P. Fraser, D. E. Shea, M. Khan, A. Bahinski, G. A. Hamilton and D. E. Ingber, *Nat. Protoc.*, 2013, **8**, 2135–2157.
57 H. Kimura, Y. Sakai and T. Fujii, *Drug Metab. Pharmacokinet.*, 2018, **33**, 43–48.
58 M. T. Nelson, M. R. Charbonneau, H. G. Coia, M. J. Castillo, C. Holt, E. S. Greenwood, P. J. Robinson, E. A. Merrill, D. Lubkowicz and C. A. Mauzy, *Nat. Commun.*, 2021, **12**, 2805.
59 K. J. Pocock, X. Gao, C. Wang, C. Priest, C. A. Prestidge, K. Mawatari, T. Kitamori and B. Thierry, *J. Micro/Nanolithogr., MEMS, MOEMS*, 2016, **15**, 044502.
60 D. Gao, H. Liu, Y. Jiang, J. M. Lin, D. Gao, H. Liu and Y. Jiang, *TrAC, Trends Anal. Chem.*, 2012, **35**, 150–164.
61 E. G. Yilmaz, N. Hacıosmanoğlu, S. B. U. Jordi, B. Yilmaz and F. Inci, *Trends Biotechnol.*, 2024, DOI: **10.1016/j.tibtech.2024.10.002**.
62 H. Wang, X. Li, P. Shi, X. You and G. Zhao, *Mater. Today Bio*, 2024, **26**, 101079.
63 L. Wang, J. Han, W. Su, A. Li, W. Zhang, H. Li, H. Hu, W. Song, C. Xu and J. Chen, *Microsyst. Nanoeng.*, 2023, **9**, 1–13.
64 S. Kang, D. Kim, J. Lee, S. Takayama and J. Y. Park, *Adv. Healthcare Mater.*, 2021, **10**, 2001284.

65 J. Barrila, J. Yang, A. Crabbé, S. F. Sarker, Y. Liu, C. M. Ott, M. A. Nelman-Gonzalez, S. J. Clemett, S. D. Nydam, R. J. Forsyth, R. R. Davis, B. E. Crucian, H. Quiriarte, K. L. Roland, K. Brenneman, C. Sams, C. Loscher and C. A. Nickerson, *npj Microgravity*, 2017, **3**, 10.
66 Q. Ramadan and L. Jing, *Biomed. Microdevices*, 2016, **18**, 1–9.
67 C. A. M. Fois, A. Schindeler, P. Valtchev and F. Dehghani, *Biomed. Microdevices*, 2021, **23**, 55.
68 W. Shin and H. J. Kim, *Nat. Protoc.*, 2022, **17**, 910–939.
69 S. Jalili-Firoozinezhad, F. S. Gazzaniga, E. L. Calamari, D. M. Camacho, C. W. Fadel, A. Bein, B. Swenor, B. Nestor, M. J. Cronce, A. Tovaglieri, O. Levy, K. E. Gregory, D. T. Breault, J. M. S. Cabral, D. L. Kasper, R. Novak and D. E. Ingber, *Nat. Biomed. Eng.*, 2019, **3**, 520–531.
70 H. J. Kim and D. E. Ingber, *Integr. Biol.*, 2013, **5**, 1130.
71 L. Zheng, C. J. Kelly and S. P. Colgan, *Am. J. Physiol.: Cell Physiol.*, 2015, **309**, C350–C360.
72 N. Sasaki, K. Miyamoto, K. M. Maslowski, H. Ohno, T. Kanai and T. Sato, *Gastroenterology*, 2020, **159**, 388–390.
73 J. D. Long and R. C. Orlando, *Am. J. Gastroenterol.*, 1999, **94**, 2818.
74 H. B. Gelberg, *Toxicol. Pathol.*, 2014, **42**, 54–66.
75 A. Maroni, L. Zema, M. D. Del Curto, A. Foppoli and A. Gazzaniga, *Adv. Drug Delivery Rev.*, 2012, **64**, 540–556.
76 J. H. Sung, J. Yu, D. Luo, M. L. Shuler and J. C. March, *Lab Chip*, 2011, **11**, 389–392.
77 K.-Y. Shim, D. Lee, J. Han, N.-T. Nguyen, S. Park and J. H. Sung, *Biomed. Microdevices*, 2017, **19**, 37.
78 L. Wang, S. K. Murthy, W. H. Fowle, G. A. Barabino and R. L. Carrier, *Biomaterials*, 2009, **30**, 6825–6834.
79 N. Ashammakhi, R. Nasiri, N. R. D. Barros, P. Tebon, J. Thakor, M. Goudie, A. Shamloo, M. G. Martin and A. Khademhosseini, *Biomaterials*, 2020, **255**, 120196.
80 Y. Chen, W. Zhou, T. Roh, M. K. Estes and D. L. Kaplan, *PLoS One*, 2017, **12**, 1–20.
81 S. C. Emencheta, C. V. Olovo, O. C. Eze, C. F. Kalu, D. P. Berebon, E. B. Onuigbo, M. M. D. C. Vila, V. M. Balcão and A. A. Attama, *Pharmaceutics*, 2023, **15**, 2416.
82 H. J. Kim, D. Huh, G. Hamilton and D. E. Ingber, *Lab Chip*, 2012, **12**, 2165–2174.
83 M. Marzorati, B. Vanhoecke, T. De Ryck, M. Sadaghian Sadabad, I. Pinheiro, S. Possemiers, P. Van den Abbeele, L. Derycke, M. Bracke, J. Pieters, T. Hennebel, H. J. Harmsen, W. Verstraete and T. Van de Wiele, *BMC Microbiol.*, 2014, **14**, 133.
84 H. J. Kim, H. Li, J. J. Collins and D. E. Ingber, *Proc. Natl. Acad. Sci. U. S. A.*, 2016, **113**, E7–E15.
85 G. P. Donaldson, S. M. Lee and S. K. Mazmanian, *Nat. Rev. Microbiol.*, 2015, **14**, 20–32.
86 W. Shin, A. Wu, M. W. Massidda, C. Foster, N. Thomas, D.-W. Lee, H. Koh, Y. Ju, J. Kim and H. J. Kim, *Front. Bioeng. Biotechnol.*, 2019, **7**, 13.
87 M. S. Jeon, Y. Y. Choi, S. J. Mo, J. H. Ha, Y. S. Lee, H. U. Lee, S. D. Park, J.-J. Shim, J.-L. Lee and B. G. Chung, *Nano Convergence*, 2022, **9**, 8.
88 R. Villenave, S. Q. Wales, T. Hamkins-Indik, E. Papafragkou, J. C. Weaver, T. C. Ferrante, A. Bahinski, C. A. Elkins, M. Kulka and D. E. Ingber, *PLoS One*, 2017, **12**, e0169412.
89 S. Min, N. Than, Y. C. Shin, G. Hu, W. Shin, Y. M. Ambrosini and H. J. Kim, *Sci. Rep.*, 2022, **12**, 22641.
90 V. De Gregorio, C. Sgambato, F. Urciuolo, R. Vecchione, P. A. Netti and G. Imparato, *Biomaterials*, 2022, **286**, 121573.
91 W. Shin and H. J. Kim, *Proc. Natl. Acad. Sci. U. S. A.*, 2018, **115**, E10539–E10547.
92 D. S. K. Brasino, S. D. Speese, K. Schilling, C. E. Schutt and M. C. Barton, *Adv. Sci.*, 2024, **11**, 2309220.
93 P. Shah, J. V. Fritz, E. Glaab, M. S. Desai, K. Greenhalgh, A. Frachet, M. Niegowska, M. Estes, C. Jäger, C. Seguin-Devaux, F. Zenhausern and P. Wilmes, *Nat. Commun.*, 2016, **7**, 11535.
94 M. Maurer, M. S. Gresnigt, A. Last, T. Wollny, F. Berlinghof, R. Pospich, Z. Cseresnyes, A. Medyukhina, K. Graf, M. Gröger, M. Raasch, F. Siwczak, S. Nietzsche, I. D. Jacobsen, M. T. Figge, B. Hube, O. Huber and A. S. Mosig, *Biomaterials*, 2019, **220**, 119396.
95 B. Jing, K. Xia, C. Zhang, S. Jiao, L. Zhu, J. Wei, Z. A. Wang, N. Chen, P. Tu, J. Li and Y. Du, *Front. Cell Dev. Biol.*, 2022, **10**, 877892.
96 B. Jing, Z. A. Wang, C. Zhang, Q. Deng, J. Wei, Y. Luo, X. Zhang, J. Li and Y. Du, *Front. Bioeng. Biotechnol.*, 2020, **8**, 272.
97 Y. Guo, R. Luo, Y. Wang, P. Deng, T. Song, M. Zhang, P. Wang, X. Zhang, K. Cui, T. Tao, Z. Li, W. Chen, Y. Zheng and J. Qin, *Sci. Bull.*, 2021, **66**, 783–793.
98 W. Zhao, Y. Yao, T. Zhang, H. Lu, X. Zhang, L. Zhao, X. Chen, J. Zhu, G. Sui and W. Zhao, *Front. Bioeng. Biotechnol.*, 2022, **10**, 1035647.
99 J. Zhang, Y. J. Huang, J. Y. Yoon, J. Kemmitt, C. Wright, K. Schneider, P. Sphabmixay, V. Hernandez-Gordillo, S. J. Holcomb, B. Bhushan, G. Rohatgi, K. Benton, D. Carpenter, J. C. Kester, G. Eng, D. T. Breault, O. Yilmaz, M. Taketani, C. A. Voigt, R. L. Carrier, D. L. Trumper and L. G. Griffith, *Med.*, 2021, **2**, 74–98.
100 F. S. Gazzaniga, D. M. Camacho, M. Wu, M. F. Silva Palazzo, A. L. M. Dinis, F. N. Grafton, M. J. Cartwright, M. Super, D. L. Kasper and D. E. Ingber, *Front. Cell. Infect. Microbiol.*, 2021, **11**, 638014.
101 J. K. Stauffer, A. J. Scarzello, Q. Jiang and R. H. Wiltrout, *Hepatology*, 2012, **56**, 1567–1574.
102 J. Da Costa Lopes, L. F. M. Falcão, A. J. Martins Filho, M. L. G. Carvalho, C. C. H. Mendes, F. A. Olímpio, V. Do Socorro Cabral Miranda, L. C. Dos Santos, J. O. Chiang, A. C. R. Cruz, V. C. A. Galúcio, R. Do Socorro Da Silva Azevedo, L. C. Martins, M. I. S. Duarte, J. R. De Sousa, P. F. Da Costa Vasconcelos and J. A. S. Quaresma, *Viruses*, 2022, **14**, 1204.
103 C. T. Ho, R. Z. Lin, R. J. Chen, C. K. Chin, S. E. Gong, H. Y. Chang, H. L. Peng, L. Hsu, T. R. Yew, S. F. Chang and C. H. Liu, *Lab Chip*, 2013, **13**, 3578–3587.

104 R. S. McCuskey, W. Ekataksin, A. V. LeBouton, J. Nishida, M. K. McCuskey, D. McDonnell, C. Williams, N. W. Bethea, B. Dvorak and O. Koldovsky, *Anat. Rec., Part A*, 2003, **275**, 1019–1030.
105 A. Ehrlich, D. Duche, G. Ouedraogo and Y. Nahmias, *Annu. Rev. Biomed. Eng.*, 2019, **21**, 219–239.
106 F. Braet and E. Wisse, *Comp. Hepatol.*, 2002, **1**, 1.
107 P. Godoy, N. J. Hewitt, U. Albrecht, M. E. Andersen, N. Ansari, S. Bhattacharya, J. G. Bode, J. Bolleyn, C. Borner, J. Böttger, A. Braeuning, R. A. Budinsky, B. Burkhardt, N. R. Cameron, G. Camussi, C.-S. Cho, Y.-J. Choi, J. Craig Rowlands, U. Dahmen, G. Damm, O. Dirsch, M. T. Donato, J. Dong, S. Dooley, D. Drasdo, R. Eakins, K. S. Ferreira, V. Fonsato, J. Fraczek, R. Gebhardt, A. Gibson, M. Glanemann, C. E. P. Goldring, M. J. Gómez-Lechón, G. M. M. Groothuis, L. Gustavsson, C. Guyot, D. Hallifax, S. Hammad, A. Hayward, D. Häussinger, C. Hellerbrand, P. Hewitt, S. Hoehme, H.-G. Holzhütter, J. B. Houston, J. Hrach, K. Ito, H. Jaeschke, V. Keitel, J. M. Kelm, B. Kevin Park, C. Kordes, G. A. Kullak-Ublick, E. L. LeCluyse, P. Lu, J. Luebke-Wheeler, A. Lutz, D. J. Maltman, M. Matz-Soja, P. McMullen, I. Merfort, S. Messner, C. Meyer, J. Mwinyi, D. J. Naisbitt, A. K. Nussler, P. Olinga, F. Pampaloni, J. Pi, L. Pluta, S. A. Przyborski, A. Ramachandran, V. Rogiers, C. Rowe, C. Schelcher, K. Schmich, M. Schwarz, B. Singh, E. H. K. Stelzer, B. Stieger, R. Stöber, Y. Sugiyama, C. Tetta, W. E. Thasler, T. Vanhaecke, M. Vinken, T. S. Weiss, A. Widera, C. G. Woods, J. J. Xu, K. M. Yarborough and J. G. Hengstler, *Arch. Toxicol.*, 2013, **87**, 1315–1530.
108 A. M. Andez and P. S. Amenta, *FASEB J.*, 1995, **9**, 1401–1410.
109 A. Treyer and A. Müsch, *Compr. Physiol.*, 2013, **3**, 243–287.
110 E. M. Materne, A. G. Tonevitsky and U. Marx, *Lab Chip*, 2013, **13**, 3481–3495.
111 K. Du, S. Li, C. Li, P. Li, C. Miao, T. Luo, B. Qiu and W. Ding, *Acta Biomater.*, 2021, **134**, 228–239.
112 S. Baek, H.-S. Ha, J. S. Park, M. J. Cho, H.-S. Kim, S. E. Yu, S. Chung, C. Kim, J. Kim, J. Y. Lee, Y. Lee, H. Kim, Y. Nam, S. Cho, K. Lee, J. K. Yoon, J. S. Choi, D. H. Han and H.-J. Sung, *Nat. Commun.*, 2024, **15**, 5117.
113 K. Zeilinger, N. Freyer, G. Damm, D. Seehofer and F. Knöspel, *Exp. Biol. Med.*, 2016, **241**, 1684–1698.
114 Q. Zhou, L. Fan and J. Li, *Artif. Liver*, 2011, **4**, 73–94.
115 B. R. Lee, J. W. Hwang, Y. Y. Choi, S. F. Wong, Y. H. Hwang, D. Y. Lee and S. H. Lee, *Biomaterials*, 2012, **33**, 837–845.
116 M. J. Powers, D. M. Janigian, K. E. Wack, C. S. Baker, D. B. Stolz and L. G. Griffith, *Tissue Eng.*, 2002, **8**, 499–513.
117 M. J. Powers, D. M. Janigian, K. E. Wack, C. S. Baker, D. B. Stolz and L. G. Griffith, *Tissue Eng.*, 2002, **8**, 499–513.
118 A. W. Tilles, H. Baskaran, P. Roy, M. L. Yarmush and M. Toner, *Biotechnol. Bioeng.*, 2001, **73**, 379–389.
119 A. J. Strain and J. M. Neuberger, *Science*, 2002, **295**, 1005–1009.
120 D. P. Williams, R. Shipley, M. J. Ellis, S. Webb, J. Ward, I. Gardner and S. Creton, *Toxicol. Res.*, 2013, **2**, 40–59.
121 G. H. Underhill and S. R. Khetani, *Cell. Mol. Gastroenterol. Hepatol.*, 2018, **5**, 426–439.
122 L. C. Snouber, A. Bunescu, M. Naudot, C. Legallais, C. Brochot, M. E. Dumas, B. Elena-Herrmann and E. Leclerc, *Toxicol. Sci.*, 2013, **132**, 8–20.
123 H. Andersson and A. Van Den Berg, *Curr. Opin. Biotechnol*, 2004, **15**, 44–49.
124 D. Castel, A. Pitaval, M. A. Debily and X. Gidrol, *Drug Discovery Today*, 2006, **11**, 616–622.
125 J. Y. Park and L. J. Kricka, *Lab Chip*, 2007, **7**, 547–549.
126 K.-J. Jang, M. A. Otieno, J. Ronxhi, H.-K. Lim, L. Ewart, K. R. Kodella, D. B. Petropolis, G. Kulkarni, J. E. Rubins, D. Conegliano, J. Nawroth, D. Simic, W. Lam, M. Singer, E. Barale, B. Singh, M. Sonee, A. J. Streeter, C. Manthey, B. Jones, A. Srivastava, L. C. Andersson, D. Williams, H. Park, R. Barrile, J. Sliz, A. Herland, S. Haney, K. Karalis, D. E. Ingber and G. A. Hamilton, *Sci. Transl. Med.*, 2019, **11**, eaax5516.
127 V. N. Goral and P. K. Yuen, *Ann. Biomed. Eng.*, 2012, **40**, 1244–1254.
128 M. Hegde, R. Jindal, A. Bhushan, S. S. Bale, W. J. McCarty, I. Golberg, O. B. Usta and M. L. Yarmush, *Lab Chip*, 2014, **14**, 2033–2039.
129 L. Ewart, A. Apostolou, S. A. Briggs, C. V. Carman, J. T. Chaff, A. R. Heng, S. Jadalannagari, J. Janardhanan, K.-J. Jang, S. R. Joshipura, M. M. Kadam, M. Kanellias, V. J. Kujala, G. Kulkarni, C. Y. Le, C. Lucchesi, D. V. Manatakis, K. K. Maniar, M. E. Quinn, J. S. Ravan, A. C. Rizos, J. F. K. Sauld, J. D. Sliz, W. Tien-Street, D. R. Trinidad, J. Velez, M. Wendell, O. Irrechukwu, P. K. Mahalingaiah, D. E. Ingber, J. W. Scannell and D. Levner, *Commun. Med.*, 2022, **2**, 1–16.
130 M. Rezvani, L. Vallier and A. Guillot, *Cell. Mol. Gastroenterol. Hepatol.*, 2023, **15**, 1135–1145.
131 E. Moradi, S. Jalili-Firoozinezhad and M. Solati-Hashjin, *Acta Biomater.*, 2020, **116**, 67–83.
132 M. Liu, Y. Xiang, Y. Yang, X. Long, Z. Xiao, Y. Nan, Y. Jiang, Y. Qiu, Q. Huang and K. Ai, *Biosens. Bioelectron.*, 2022, **218**, 114758.
133 P. J. Lee, P. J. Hung and L. P. Lee, *Biotechnol. Bioeng.*, 2007, **97**, 1340–1346.
134 J. Deng, X. Zhang, Z. Chen, Y. Luo, Y. Lu, T. Liu, Z. Wu, Y. Jin, W. Zhao and B. Lin, *Biomicrofluidics*, 2019, **13**, 024101.
135 Y. Du, N. Li, H. Yang, C. Luo, Y. Gong, C. Tong, Y. Gao, S. Lü and M. Long, *Lab Chip*, 2017, **17**, 782–794.
136 K. Rennert, S. Steinborn, M. Gröger, B. Ungerböck, A. M. Jank, J. Ehgartner, S. Nietzsche, J. Dinger, M. Kiehntopf, H. Funke, F. T. Peters, A. Lupp, C. Gärtner, T. Mayr, M. Bauer, O. Huber and A. S. Mosig, *Biomaterials*, 2015, **71**, 119–131.

137 M. Raasch, K. Rennert, T. Jahn, S. Peters, T. Henkel, O. Huber, I. Schulz, H. Becker, S. Lorkowski, H. Funke and A. Mosig, *Biofabrication*, 2015, **7**, 15013.
138 S. Mi, X. Yi, Z. Du, Y. Xu and W. Sun, *Biofabrication*, 2018, **10**, 025010.
139 M. Verhulsel, M. Vignes, S. Descroix, L. Malaquin, D. M. Vignjevic and J. L. Viovy, *Biomaterials*, 2014, **35**, 1816–1832.
140 Y. S. Chen, C. K. Tung, T. H. Dai, X. Wang, C. T. Yeh, S. K. Fan and C. H. Liu, *Sens. Actuators, B*, 2021, **343**, 130159.
141 Y. Du, N. Li, H. Yang, C. Luo, Y. Gong, C. Tong, Y. Gao, S. Lü and M. Long, *Lab Chip*, 2017, **17**, 782–794.
142 F. Tonon, G. G. Giobbe, A. Zambon, C. Luni, O. Gagliano, A. Floreani, G. Grassi and N. Elvassore, *Sci. Rep.*, 2019, **9**, 13557.
143 A. A. Banaeiyan, J. Theobald, J. Paukštyte, S. Wölfl, C. B. Adiels and M. Goksör, *Biofabrication*, 2017, **9**, 015014.
144 K. E. Cottier, D. Bhalerao, C. Lewis, J. Gaffney and S. A. Heyward, *Sci. Rep.*, 2023, **13**, 15837.
145 B. R. Ware, J. S. Liu, C. P. Monckton, K. R. Ballinger and S. R. Khetani, *Toxicol. Sci.*, 2021, **181**, 90–104.
146 J. W. Allen, T. Hassanein and S. N. Bhatia, *Hepatology*, 2001, **34**, 447–455.
147 J. F. Patzer Ii, *Ann. N. Y. Acad. Sci.*, 2001, **944**, 320–333.
148 F. L. A. Willekens, J. M. Werre, J. K. Kruijt, B. Roerdinkholder-Stoelwinder, Y. A. M. Groenen-Döpp, A. G. Van Den Bos, G. J. C. G. M. Bosman and T. J. C. Van Berkel, *Blood*, 2005, **105**, 2141–2145.
149 S. B. Leite, T. Roosens, A. El Taghdouini, I. Mannaerts, A. J. Smout, M. Najimi, E. Sokal, F. Noor, C. Chesne and L. A. van Grunsven, *Biomaterials*, 2016, **78**, 1–10.
150 J. LeCouter, D. R. Moritz, B. Li, G. L. Phillips, X. H. Liang, H.-P. Gerber, K. J. Hillan and N. Ferrara, *Science*, 2003, **299**, 890–893.
151 S. Kidambi, L. Sheng, M. L. Yarmush, M. Toner, I. Lee and C. Chan, *Macromol. Biosci.*, 2007, **7**, 344–353.
152 M. Yamato, O. H. Kwon, M. Hirose, A. Kikuchi and T. Okano, *J. Biomed. Mater. Res.*, 2001, **55**, 137–140.
153 S. P. Maher, R. B. Crouse, A. J. Conway, E. C. Bannister, A. K. H. Achyuta, A. Y. Clark, F. L. Sinatra, J. D. Cuiffi, J. H. Adams, D. E. Kyle and W. M. Saadi, *Biomed. Microdevices*, 2014, **16**, 727–736.
154 L. Prodanov, R. Jindal, S. S. Bale, M. Hegde, W. J. Mccarty, I. Golberg, A. Bhushan, M. L. Yarmush and O. B. Usta, *Biotechnol. Bioeng.*, 2016, **113**, 241–246.
155 J. Deng, W. Wei, Z. Chen, B. Lin, W. Zhao, Y. Luo and X. Zhang, *Micromachines*, 2019, **10**, 1–26.
156 J. W. Allen and S. N. Bhatia, *Biotechnol. Bioeng.*, 2003, **82**, 253–262.
157 J. J. Lemasters, H. Bunzendahl and R. G. Thurman, *Liver Transpl.*, 1995, **1**, 124–138.
158 F. Tonon, G. G. Giobbe, A. Zambon, C. Luni, O. Gagliano, A. Floreani, G. Grassi and N. Elvassore, *Sci. Rep.*, 2019, **9**, 1–10.
159 Y. B. Kang, J. Eo, B. Bulutoglu, M. L. Yarmush and O. B. Usta, *Biotechnol. Bioeng.*, 2020, **117**, 763–775.
160 Y. Tanaka, M. Yamato, T. Okano, T. Kitamori and K. Sato, *Meas. Sci. Technol.*, 2006, **17**, 3167–3170.
161 S. Kidambi, R. S. Yarmush, E. Novik, P. Chao, M. L. Yarmush and Y. Nahmias, *Proc. Natl. Acad. Sci. U. S. A.*, 2009, **106**, 15714–15719.
162 S. R. Khetani and S. N. Bhatia, *Nat. Biotechnol.*, 2008, **26**, 120–126.
163 L. A. Low, C. Mummery, B. R. Berridge, C. P. Austin and D. A. Tagle, *Nat. Rev. Drug Discovery*, 2021, **20**, 345–361.
164 S. G. Kang, Y. Y. Choi, S. J. Mo, T. H. Kim, J. H. Ha, D. K. Hong, H. Lee, S. D. Park, J.-J. Shim, J.-L. Lee and B. G. Chung, *Nano Convergence*, 2023, **10**, 5.
165 I. Maschmeyer, A. K. Lorenz, K. Schimek, T. Hasenberg, A. P. Ramme, J. Hübner, M. Lindner, C. Drewell, S. Bauer, A. Thomas, N. S. Sambo, F. Sonntag, R. Lauster and U. Marx, *Lab Chip*, 2015, **15**, 2688–2699.
166 Z. Li, W. Su, Y. Zhu, T. Tao, D. Li, X. Peng and J. Qin, *Biomicrofluidics*, 2017, **11**, 034114.
167 J. Jeon, S. H. Lee, D. Kim and J. H. Sung, *Biotechnol. Prog.*, 2021, **37**, e3121.
168 N. Xu, H. Lin, J. M. Lin, J. Cheng, P. Wang and L. Lin, *Anal. Chem.*, 2023, **95**, 17064–17072.
169 P. M. Van Midwoud, M. T. Merema, E. Verpoorte and G. M. M. Groothuis, *Lab Chip*, 2010, **10**, 2778–2786.
170 H. J. Chen, P. Miller and M. L. Shuler, *Lab Chip*, 2018, **18**, 2036–2046.
171 S. Y. Lee and J. H. Sung, *Biotechnol. Bioeng.*, 2018, **115**, 2817–2827.
172 N. Tsamandouras, W. L. K. Chen, C. D. Edington, C. L. Stokes, L. G. Griffith and M. Cirit, *AAPS J.*, 2017, **19**, 1499–1512.
173 W. L. Chen, C. Edington, E. Suter, J. Yu, J. J. Velazquez, J. G. Velazquez, M. Shockley, E. M. Large, R. Venkataramanan, D. J. Hughes, C. L. Stokes, D. L. Trumper, R. L. Carrier, M. Cirit, L. G. Griffith and D. A. Lauffenburger, *Biotechnol. Bioeng*, 2017, **114**, 2648–2659.
174 T. Bricks, P. Paullier, A. Legendre, M. J. Fleury, P. Zeller, F. Merlier, P. M. Anton and E. Leclerc, *Toxicol. in Vitro*, 2014, **28**, 885–895.
175 N. Milani, N. Parrott, D. Ortiz Franyuti, P. Godoy, A. Galetin, M. Gertz and S. Fowler, *Lab Chip*, 2022, **22**, 2853–2868.
176 M. B. Esch, G. J. Mahler, T. Stokol and M. L. Shuler, *Lab Chip*, 2014, **14**, 3081–3092.
177 X. Duan, L. Zheng, X. Zhang, B. Wang, M. Xiao, W. Zhao, S. Liu and G. Sui, *ACS Sens.*, 2020, **5**, 3483–3492.
178 P. De Haan, M. A. Ianovska, K. Mathwig, G. A. A. Van Lieshout, V. Triantis, H. Bouwmeester and E. Verpoorte, *Lab Chip*, 2019, **19**, 1599–1609.
179 R. Kim and J. H. Sung, *Adv. Healthcare Mater.*, 2024, **13**, 2302777.
180 L. Boeri, L. Izzo, L. Sardelli, M. Tunesi, D. Albani and C. Giordano, *Bioengineering*, 2019, **6**, 91.

181 Y. Guo, X. Chen, P. Gong, G. Li, W. Yao and W. Yang, *Int. J. Mol. Sci.*, 2023, **24**, 4089.
182 J. Jeon, N. Choi, S. H. Lee and J. H. Sung, *Biomed. Microdevices*, 2020, **22**, 65.
183 A. Skardal, M. Devarasetty, S. Forsythe, A. Atala and S. Soker, *Biotechnol. Bioeng.*, 2016, **113**, 2020–2032.
184 C. Quintard, E. Tubbs, G. Jonsson, J. Jiao, J. Wang, N. Werschler, C. Laporte, A. Pitaval, T.-S. Bah, G. Pomeranz, C. Bissardon, J. Kaal, A. Leopoldi, D. A. Long, P. Blandin, J.-L. Achard, C. Battail, A. Hagelkruys, F. Navarro, Y. Fouillet, J. M. Penninger and X. Gidrol, *Nat. Commun.*, 2024, **15**, 1452.
185 L. A. Vernetti, N. Senutovitch, R. Boltz, R. DeBiasio, T. Ying Shun, A. Gough and D. L. Taylor, *Exp. Biol. Med.*, 2016, **241**, 101–114.
186 A. S. Moghaddam, Z. S. Moghaddam, S. M. Davachi, E. Sarikhani, S. N. Mahand, H. A. Khonakdar, Z. Bagher and N. Ashammakhi, *Mater. Chem. Front.*, 2022, **6**, 3633–3661.
187 E. Ferrari, E. Monti, C. Cerutti, R. Visone, P. Occhetta, L. G. Griffith and M. Rasponi, *Biomicrofluidics*, 2023, **17**, 064103.
188 K. Yoshimoto, K. Maki, T. Adachi and K. Kamei, *Tissue Eng., Part A*, 2024, **30**, 426–439.
189 J. Lee, J. H. Choi and H. J. Kim, *Expert Rev. Gastroenterol. Hepatol.*, 2016, **10**, 883–885.
190 H. J. Kim, D. Huh, G. Hamilton and D. E. Ingber, *Lab Chip*, 2012, **12**, 2165–2174.
191 D. E. Ingber, *Cell*, 2016, **164**, 1105–1109.
192 C. Beaurivage, E. Naumovska, Y. X. Chang, E. D. Elstak, A. Nicolas, H. Wouters, G. van Moolenbroek, H. L. Lanz, S. J. Trietsch, J. Joore, P. Vulto, R. A. J. Janssen, K. S. Erdmann, J. Stallen and D. Kurek, *Int. J. Mol. Sci.*, 2019, **20**, 5661.
193 A. Bein, C. W. Fadel, B. Swenor, W. Cao, R. K. Powers, D. M. Camacho, A. Naziripour, A. Parsons, N. LoGrande, S. Sharma, S. Kim, S. Jalili-Firoozinezhad, J. Grant, D. T. Breault, J. Iqbal, A. Ali, L. A. Denson, S. R. Moore, R. Prantil-Baun, G. Goyal and D. E. Ingber, *Nat. Biomed. Eng.*, 2022, **6**, 1236–1247.
194 F. Yu, R. Deng, W. Hao Tong, L. Huan, N. C. Way, A. IslamBadhan, C. Iliescu and H. Yu, *Sci. Rep.*, 2017, **7**, 14528.
195 I. Maschmeyer, T. Hasenberg, A. Jaenicke, M. Lindner, A. K. Lorenz, J. Zech, L. A. Garbe, F. Sonntag, P. Hayden, S. Ayehunie, R. Lauster, U. Marx and E. M. Materne, *Eur. J. Pharm. Biopharm.*, 2015, **95**, 77–87.
196 J. Kahn, P. J. Tofilon and K. Camphausen, *Radiat. Oncol.*, 2012, **7**, 1–5.
197 L. Zhao, F. Zhang, X. Ding, G. Wu, Y. Y. Lam, X. Wang, H. Fu, X. Xue, C. Lu, J. Ma, L. Yu, C. Xu, Z. Ren, Y. Xu, S. Xu, H. Shen, X. Zhu, Y. Shi, Q. Shen, W. Dong, R. Liu, Y. Ling, Y. Zeng, X. Wang, Q. Zhang, J. Wang, L. Wang, Y. Wu, B. Zeng, H. Wei, M. Zhang, Y. Peng and C. Zhang, *Science*, 2018, **359**, 1151–1156.
198 C. Ma, M. Han, B. Heinrich, Q. Fu, Q. Zhang, M. Sandhu, D. Agdashian, M. Terabe, J. A. Berzofsky, V. Fako, T. Ritz, T. Longerich, C. M. Theriot, J. A. McCulloch, S. Roy, W. Yuan, V. Thovarai, S. K. Sen, M. Ruchirawat, F. Korangy, X. W. Wang, G. Trinchieri and T. F. Greten, *Science*, 2018, **360**, eaan5931.
199 L. Zhao, *Nat. Rev. Microbiol.*, 2013, **11**, 639–647.
200 V. A. Pedicord, A. A. K. Lockhart, K. J. Rangan, J. W. Craig, J. Loschko, A. Rogoz, H. C. Hang and D. Mucida, *Sci. Immunol.*, 2022, **1**, eaai7732.
201 Y. Guo, Z. Li, W. Su, L. Wang, Y. Zhu and J. Qin, *Artif. Organs*, 2018, **42**, 1196–1205.
202 Y. Guo, Y. Xie and J. Qin, *Biotechnol. J.*, 2024, **19**, 2300390.
203 J. M. Donkers, J. I. Van Der Vaart and E. Van De Steeg, *Biomimetics*, 2023, **8**, 226.
204 H. Liu, G. Yin, M. S. Kohlhepp, F. Schumacher, J. Hundertmark, M. I. A. Hassan, F. Heymann, T. Puengel, B. Kleuser, A. S. Mosig, F. Tacke and A. Guillot, *Adv. Sci.*, 2024, **11**, 2403516.
205 S. Messner, I. Agarkova, W. Moritz and J. M. Kelm, *Arch. Toxicol.*, 2013, **87**, 209–213.
206 L. Docci, N. Milani, T. Ramp, A. A. Romeo, P. Godoy, D. O. Franyuti, S. Krähenbühl, M. Gertz, A. Galetin, N. Parrott and S. Fowler, *Lab Chip*, 2022, **22**, 1187–1205.
207 J. T. Huh, J. P. R. L. L. Parra, J. S. Copus, H. W. Kang, C. E. Bishop, S. Soker, S. Murphy, T. D. Shupe, J. J. Yoo, S. J. Lee and A. Atala, *Tissue Eng., Part A*, 2024, **30**, 333–341.
208 Y. Zheng, L. Ma, J. Wu, Y. Wang, X. Meng, P. Hu, Q. Liang, Y. Xie and G. Luo, *Talanta*, 2022, **241**, 123262.
209 S. A. P. Rajan, J. Sherfey, S. Ohri, L. Nichols, J. T. Smith, P. Parekh, E. P. Kadar, F. Clark, B. T. George, L. Gregory, D. Tess, J. R. Gosset, J. Liras, E. Geishecker, R. S. Obach and M. Cirit, *AAPS J.*, 2023, **25**, 102.
210 G. H. Underhill and S. R. Khetani, *APL Bioeng.*, 2019, **3**, 040902.
211 R. Veteläinen, A. Van Vliet, D. J. Gouma and T. M. Van Gulik, *Ann. Surg.*, 2007, **245**, 20–30.
212 B. Q. Starley, C. J. Calcagno and S. A. Harrison, *Hepatology*, 2010, **51**, 1820–1832.
213 M. Gori, M. C. Simonelli, S. M. Giannitelli, L. Businaro, M. Trombetta and A. Rainer, *PLoS One*, 2016, **11**, e0159729.
214 J. Lee, B. Choi, D. Y. No, G. Lee, S. R. Lee, H. Oh and S. H. Lee, *Integr. Biol.*, 2016, **8**, 302–308.
215 A. M. Ortega-Prieto, J. K. Skelton, S. N. Wai, E. Large, M. Lussignol, G. Vizcay-Barrena, D. Hughes, R. A. Fleck, M. Thursz, M. T. Catanese and M. Dorner, *Nat. Commun.*, 2018, **9**, 682.
216 M. Lucchetti, M. Kaminska, A. K. Oluwasegun, A. S. Mosig and P. Wilmes, *Curr. Opin. Endocr. Metab. Res.*, 2021, **18**, 94–101.
217 J. H. Sung, *Methods Cell Biol.*, 2020, **158**, 1–10.
218 J. Yang, Y. Hirai, K. Iida, S. Ito, M. Trumm, S. Terada, R. Sakai, T. Tsuchiya, O. Tabata and K. Kamei, *Commun. Biol.*, 2023, **6**, 310.
219 M. Jie, H. Lin, Z. He, H. Liu, H. Li and J. M. Lin, *Sci. China:Chem.*, 2018, **61**, 236–242.

220 M. Wang, Y. Sasaki, R. Sakagami, T. Minamikawa, M. Tsuda, R. Ueno, S. Deguchi, R. Negoro, K. So, Y. Higuchi, R. Yokokawa, K. Takayama and F. Yamashita, *ACS Biomater. Sci. Eng.*, 2024, **10**, 4635–4644.
221 Y. Yu, B. Sun, X. Ye, Y. Wang, M. Zhao, J. Song, X. Geng, U. Marx, B. Li and X. Zhou, *Food Chem. Toxicol.*, 2024, **193**, 115016.
222 A. Mata, A. J. Fleischman and S. Roy, *Biomed. Microdevices*, 2005, **7**, 281–293.
223 R. Gomez-Sjoberg, A. A. Leyrat, B. T. Houseman, K. Shokat and S. R. Quake, *Anal. Chem.*, 2010, **82**, 8954–8960.
224 M. W. Toepke and D. J. Beebe, *Lab Chip*, 2006, **6**, 1484–1486.
225 J. D. Wang, N. J. Douville, S. Takayama and M. Elsayed, *Ann. Biomed. Eng.*, 2012, **40**, 1862–1873.
226 K. Domansky, J. D. Sliz, N. Wen, C. Hinojosa, G. Thompson, J. P. Fraser, T. Hamkins-Indik, G. A. Hamilton, D. Levner and D. E. Ingber, *Microfluid. Nanofluid.*, 2017, **21**, 1–12.
227 M. J. Mondrinos, Y. S. Yi, N. K. Wu, X. Ding and D. Huh, *Lab Chip*, 2017, **17**, 3146–3158.
228 H. Sun, E. C. Y. Chow, S. Liu, Y. Du and K. S. Pang, *Expert Opin. Drug Metab. Toxicol.*, 2008, **4**, 395–411.
229 R. R. Nadkarni, S. Abed, B. J. Cox, S. Bhatia, J. T. Lau, M. G. Surette and J. S. Draper, *Stem Cell Rep.*, 2017, **9**, 897–912.
230 N. Ashammakhi, K. Wesseling-Perry, A. Hasan, E. Elkhammas and Y. S. Zhang, *Kidney Int.*, 2018, **94**, 1073–1086.
231 P. Brun, S. Gobbo, V. Caputi, L. Spagnol, G. Schirato, M. Pasqualin, E. Levorato, G. Palù, M. C. Giron and I. Castagliuolo, *Mol. Cell. Neurosci.*, 2015, **68**, 24–35.
232 E. E. Benarroch, *Neurology*, 2007, **69**, 1953–1957.
233 F. Zhang, Y. Zhu, J. Chen, W. Kuang, R. Huang, F. Duan, Y. Li, L. Wang, H. Qiu, X. Chen, J. Ming, P. Liu, Y. Du, S. C. N. Chang, L. Chen and J. Na, *Biomaterials*, 2021, **271**, 120713.
234 H. A. Stone, A. D. Stroock and A. Ajdari, *Annu. Rev. Fluid Mech.*, 2004, **36**, 381–411.
235 S. R. Shin, T. Kilic, Y. S. Zhang, H. Avci, N. Hu, D. Kim, C. Branco, J. Aleman, S. Massa, A. Silvestri, J. Kang, A. Desalvo, M. A. Hussaini, S.-K. Chae, A. Polini, N. Bhise, M. A. Hussain, H. Lee, M. R. Dokmeci and A. Khademhosseini, *Adv. Sci.*, 2017, **4**, 1600522.
236 A. R. D. Germain, *Physiol. Behav.*, 2017, **176**, 139–148.
237 J. P. Wikswo, F. E. Block, D. E. Cliffel, C. R. Goodwin, C. C. Marasco, D. A. Markov, D. L. McLean, J. A. McLean, J. R. McKenzie, R. S. Reiserer, P. C. Samson, D. K. Schaffer, K. T. Seale and S. D. Sherrod, *IEEE Trans. Biomed. Eng.*, 2013, **60**, 682–690.
238 Q. Ramadan and M. Zourob, *Biomicrofluidics*, 2020, **14**, 041501.
239 K. Fabre, B. Berridge, W. R. Proctor, S. Ralston, Y. Will, S. W. Baran, G. Yoder and T. R. V. Vleet, *Lab Chip*, 2020, **20**, 1049–1057.
240 A. G. Monteduro, S. Rizzato, G. Caragnano, A. Trapani, G. Giannelli and G. Maruccio, *Biosens. Bioelectron.*, 2023, **231**, 115271.
241 D. Kumar, R. Nadda and R. Repaka, *Med. Biol. Eng. Comput.*, 2024, **62**, 1925–1957.
242 R. Kim and J. H. Sung, *Biomicrofluidics*, 2024, **18**, 031507.
243 V. De Gregorio, M. Telesco, B. Corrado, V. Rosiello, F. Urciuolo, P. A. Netti and G. Imparato, *Front. Bioeng. Biotechnol.*, 2020, **8**, 163.
244 Y. Xiang, H. Wen, Y. Yu, M. Li, X. Fu and S. Huang, *J. Tissue Eng.*, 2020, **11**, 2041731420965318.
245 V. Mehta, G. Karnam and V. Madgula, *Mater. Today Bio*, 2024, **27**, 101143.

